HHS Public Access

Author manuscript

*Brain Struct Funct*. Author manuscript; available in PMC 2020 June 29.

Published in final edited form as:

*Brain Struct Funct*. 2019 January ; 224(1): 315–336. doi:10.1007/s00429-018-1776-0.

# Modulation of olfactory-driven behavior by metabolic signals: role of the piriform cortex

**Dolly Al Koborssy**[1,4], **Brigitte Palouzier-Paulignan**[2], **Vincent Canova**[2], **Marc Thevenet**[2], **Debra Ann Fadool**[#1,3,4], **Andrée Karyn Julliard**[#2]

[1]Program in Neuroscience, The Florida State University, Tallahassee, FL, USA

[2]Univ Lyon, Université Claude Bernard Lyon1, Centre de Recherche en Neurosciences de Lyon (CRNL), INSERM U1028/CNRS UMR5292 Team Olfaction: From Coding to Memory, 50 Av. Tony Garnier, 69366 Lyon, France

[3]Institute of Molecular Biophysics, The Florida State University, Tallahassee, FL, USA

[4]Department of Biological Science, The Florida State University, Tallahassee, FL, USA

[#] These authors contributed equally to this work.

## Abstract

Olfaction is one of the major sensory modalities that regulates food consumption and is in turn regulated by the feeding state. Given that the olfactory bulb has been shown to be a metabolic sensor, we explored whether the anterior piriform cortex (aPCtx)—a higher olfactory cortical processing area—had the same capacity. Using immunocytochemical approaches, we report the localization of Kv1.3 channel, glucose transporter type 4, and the insulin receptor in the lateral olfactory tract and Layers II and III of the aPCtx. In current-clamped superficial pyramidal (SP) cells, we report the presence of two populations of SP cells: glucose responsive and non-glucose responsive. Using varied glucose concentrations and a glycolysis inhibitor, we found that insulin modulation of the instantaneous and spike firing frequency are both glucose dependent and require glucose metabolism. Using a plethysmograph to record sniffing frequency, rats microinjected with insulin failed to discriminate ratiometric enantiomers; considered a difficult task. Microinjection of glucose prevented discrimination of odorants of different chain-lengths, whereas injection of margatoxin increased the rate of habituation to repeated odor stimulation and enhanced discrimination. These data suggest that metabolic signaling pathways that are present in the aPCtx are capable of neuronal modulation and changing complex olfactory behaviors in higher olfactory centers.

✉ Andrée Karyn Julliard, karyn.julliard@univ-lyon1.fr.

**Conflict of interest** The authors declare that they have no conflict of interest.

**Research involving animals and ethical approval** All applicable international, national, and/or institutional guidelines for the care and use of animals were followed. Experimental protocols were approved by the Lyon University Animal Experimentation Committee, the French Ministry of Higher Education and Research (APAFIS#9924-20170051614351992 v1), and the Florida State University (FSU) Institutional Animal Care and Use Committee (IACUC) under protocols no. 1427 and 1733. Experiments were carried out in accordance with the European Community Council Directive of November 24, 1986 (86/609/EEC), the American Veterinary Medicine Association (AVMA), and the National Institutes of Health (NIH).

**Informed consent** This article does not contain any studies with human participants performed by any of the authors.

**Keywords**

Olfaction; Piriform; Glucose; GLUT4; Insulin; Kv1.3; Sniffing behavior

## Introduction

Olfactory perception determines the food choice of most living species whether for humans in driving appetite or animal species avoiding inappropriate foodstuffs (Dematte et al. 2013; Sachse and Beshel 2016). The first relay of olfactory information is the olfactory bulb (OB), which has interestingly been highlighted as a metabolic (Palouzier-Paulignan et al. 2012) or nutrient sensor (Julliard et al. 2017). Two important metabolic molecules, glucose and insulin, have been well defined to modulate the firing frequency of the OB primary output neurons, called mitral cells (MCs) (Fadool et al. 2000; Kuczewski et al. 2014; Tucker et al. 2013). Not only do MCs respond to changes in extracellular glucose and insulin concentration, but an imbalance in metabolic homeostasis, feeding state, or obesity can disrupt the function of the OB as a sensor (Aime et al. 2014; Fadool et al. 2011; Lacroix et al. 2015; Marks et al. 2009; Thiebaud et al. 2014). The molecular and cellular mechanisms underlying glucose and insulin sensing in the OB have been localized to MCs that express the insulin receptor (IR) (Aime et al. 2012), glucose transporter type 4 (GLUT4) (Al Koborssy et al. 2014), and the voltage-gated potassium channel, Kv1.3 (Fadool and Levitan 1998; Fadool et al. 2000). Kv1.3 channels are substrates for insulin phosphorylation (Colley et al. 2007; Fadool et al. 2000; Marks et al. 2009) whereas a decrease in Kv1.3 conductance can increase GLUT4 translocation to the membrane in a calcium-dependent manner to increase glucose uptake (Kovach et al. 2016; Li et al. 2006; Xu et al. 2004). Previously we have suggested that modulation of GLUT4 expression in the OB that is related to food intake (Al Koborssy et al. 2014) could be responsible for the difference in olfactory sensitivity observed between satiated and fasted rats (Aime et al. 2007).

While the highest insulin transport rate and highest insulin binding affinity in the brain is found in the OB (Banks et al. 1999; Baskin et al. 1983), the presence of glucose signaling proteins may be more ubiquitously distributed. Glucose sensors have been reported throughout the brain including the hypothalamus, brainstem, amygdala, septum, and hippocampus (Anand et al. 1964; Balfour et al. 2006; Oomura et al. 1969; Ren et al. 2009). Because MCs send their projections widely to higher olfactory centers, we were curious as to whether these central processing areas might serve as an extension of the metabolic or nutrient sensor reported initially in the OB. No study to our knowledge has explored the presence and connection between Kv1.3, glucose transporters, and IR in any higher olfactory centers including primary olfactory cortices, i.e., the piriform cortex.

The anterior piriform cortex (aPCtx) consists of a three-layered paleocortex. Layer I is a superficial layer containing the OB feedforward connections derived by the lateral olfactory tract (LOT), the apical dendrites of Layer II/III principal neurons, and a sparse population of local interneurons. In adult rodents, Layer I is further subdivided into two sublayers: Layer Ia contains the axonal projections of the MCs and tufted cells (TCs) at the level where the LOT terminates, and Layer Ib receives intracortical fibers mainly from the anterior olfactory

nucleus and the PCtx (Price 1973). Layer II is where densely packed glutamatergic principal neurons reside. Layer III contains a lower density of deep principal neurons and harbors a more heterogeneous population of excitatory and inhibitory neurons (Ekstrand et al. 2001; Haberly 1983; Kapur et al. 1997; Suzuki and Bekkers 2010). The principal cells of Layer II consist of excitatory superficial pyramidal and semi-lunar cells (Suzuki and Bekkers 2006). Interestingly, the aPCtx shares commonalities with the OB in terms of metabolic sensitivity and potential regulation. It receives synaptic input from both the OB and central sources (Shepherd 2004) and projects glutamatergic fibers to feeding-related areas, including the lateral hypothalamus (Blevins et al. 2004). Similar to the OB, the aPCtx expresses receptors for peptides such as the IR, and glucose transporters such as GLUT4 (El Messari et al. 2002; Hill et al. 1986; Schulingkamp et al. 2000; Unger et al. 1989; Zhou et al. 2017). A recent study showed that insulin ICV injection induced a decrease in odor-evoked responses of aPCtx pyramidal neuron activity (Zhou et al. 2017). These authors have suggested that insulin's effect on the aPCtx could be responsible for the increase in odor perception threshold similar to what we previously described in the OB (Aime et al. 2012). The aPCtx has also been reported to detect imbalances in essential amino acids in non-nutritious meals (Rudell et al. 2011). With the exception of the insulin study (Zhou et al. 2017), the functional role of metabolic signals and theirs receptors and transporters in the aPCtx, and their relationship to olfactory function remain largely unexplored.

The aPCtx is an important site of odor object synthesis. It is able to recognize a mixture of odorants as novel odors (Barnes et al. 2008), thereby playing a major role in olfactory discrimination (Wilson 2003; Wilson and Sullivan 2011). Olfactory discrimination is linked to active sampling of olfactory information that is achieved through sniffing. Sniffing is defined as rapid and repeated bouts of inhalation of volatile molecules at a frequency ranging from 4 to 12 Hz (Youngentob et al. 1987). In behaving animals, sniffing is highly dynamic, notably in frequency and flowrate (Wesson et al. 2008; Youngentob et al. 1987). Sampling a novel odorant results in reliable induction of high-frequency (6–10 Hz) sniffing (Kepecs et al. 2007; Macrides et al. 1982; Welker 1964; Wesson et al. 2008; Youngentob et al. 1987). Habituation induced by odor repetition leads to a decrease in orientation responses (Sundberg et al. 1982) and sniffing frequency (Wesson et al. 2011). In this sense, respiratory activity can be a good index of—(i) stimulus novelty detection, (ii) odor habituation or adaptation to the environment, or (iii) olfactory discrimination (Kepecs et al. 2007; Ranade et al. 2013; Rojas-Libano et al. 2014; Uchida and Mainen 2003; Welker 1964; Youngentob et al. 1987).

Herein, we investigate and confirm a novel neuromodulatory role of the aPCtx network involving metabolic signals. First, we used immunocytochemistry to map the cellular expression of the glucose transporter type 4 (GLUT4), the IR, and the voltage-gated potassium channel, Kv1.3. Next, we used patch-clamp electrophysiology to biophysically define the responsiveness of principal cells of the aPCtx to glucose and insulin. Lastly, we tested if bilateral infusion of metabolic signals into the aPCtx of Wistar rats could alter olfactory processing by examining behavioral output of sniffing rates during perception, habituation, and discrimination of several odorant mixtures.

# Methods

## Ethical approval

All applicable international, national, and/or institutional guidelines for the care and use of animals were followed. Experimental protocols were approved by the Lyon University Animal Experimentation Committee, the French Ministry of Higher Education and Research (APAFIS#9924-20170051614351992 v1), and the Florida State University (FSU) Institutional Animal Care and Use Committee (IACUC) under protocols no. 1427 and 1733. Experiments were carried out in accordance with the European Community Council Directive of November 24, 1986 (86/609/EEC), the American Veterinary Medicine Association (AVMA), and the National Institutes of Health (NIH). Care was taken at all stages to minimize stress and discomfort to the animals in compliance with the ethical principles animal ethics checklist reported by (Grundy 2015).

## Animal care

All rats (*Rattus norvegicus*, Wistar Han, Strain 003) were purchased from the company Charles River located in either Lyon, France or in Wilmington MA, USA. Rats were group housed (2–4 rats) in Plexiglas chambers on a standard 12 h/12 h light/dark inverted cycle (lights off at 08:00 a.m.) and at a constant temperature (22 ± 0.5 °C) and relative humidity (50 ± 5%). Rats of both sexes at postnatal day 20–30 were used for electrophysiology, which is reported to follow a critical period necessary for the development of the PCtx network (Franks and Isaacson 2005) and had a body weight ranging from 60 to 100 g (mean ± SEM: 80.2 ± 15.9 g). Because rats do not reach sexual maturity until 6–8 weeks of age, all our sampled female mice used for electrophysiology were anestrous. Adult male rats at 3 months of age were used sequentially for behavioral and then immunocytochemistry experiments, and had a body weight ranging from 300 to 400 g (357 ± 48 g). A total of 36 adults and 60 pups were used for this study.

For behavioral tests, animals were provided *ad libitum* access to water and Teklad global rodent diet 2018 (Harlan, Ltd./Envigo, Indianapolis, USA) for two weeks upon their arrival to the vivarium. Three weeks prior to the behavioral tests, these adult rats were gradually habituated to a 20 h/day food restriction schedule in which they had access to food from 11:00 a.m. to 3:00 p.m only. Restricted access to food limits daily fluctuations in glycemia and insulinemia (Kaul and Berdanier 1975; Sitren and Stevenson 1978) and synchronizes circadian variations of metabolic peptides within a cohort. Animals were weighed and handled daily (5 min/day) to monitor their adaptation to food restriction.

## Solutions and reagents

Blocking Solution (BS) consisted of: 0.1 M PBS (Cat # P4417, Sigma–Aldrich, Saint-Quentin Fallavier, France) (pH = 7.4), 1% bovine serum albumin (BSA, Cat # A9647, Sigma–Aldrich), and 5% normal serum from the host species of the antibody. Insulin (human recombinant insulin, 11 376 497 001 Roche Diagnostics, Indianapolis, IN, USA) was dissolved in artificial cerebral spinal fluid (ACSF, see below) at 1 qg.ml (172 nM), a concentration that was previously reported to suppress evoked currents in MCs (Fadool et al. 2000). Margatoxin (MgTx), a Kv1.3 peptide blocker, was diluted in ACSF to a working

concentration of 0.1 nM (Fadool and Levitan 1998); (Sigma-Aldrich, Atlanta, GA, USA). The concentration of D-glucose (Cat # G8270, Sigma-Aldrich, Saint-Quentin Fallavier, France specific purity grade > 99.5%) applied in behavioral experiments was retained at 10 mM. During electrophysiology experiments, D-glucose concentration varied between 0.5, 1, 5, and 10 mM, by osmotically balancing the ACSF solution to 305 mOsm with sucrose.

Dissecting solution contained (in mM): 83 NaCl, 26.2 $NaHCO_3$, 0.5 $CaCl_2$, 1 $NaH_2PO_4$, 3.3 $MgCl_2$, 10 D-glucose; 305–315 mOsm.l; pH 7.4. The bath perfusion solution (ACSF) contained (in mM): 119 NaCl, 2.5 KCl, 26.2 $NaHCO_3$, 2.5 $CaCl_2$, 1 $NaH_2PO_4$, 1.3 $MgCl_2$, 5 D-glucose; 305–315 mOsm.l; pH 7.4. The intracellular pipette solution contained (in mM): 135 K-gluconate, 10 KCl, 10 HEPES, 10 $MgCl_2$, 0.1 EGTA, 0.4 NaGTP and 2 NaATP (pH 7.3; 280–285 mOsm.l). Unless otherwise noted, salts and sugars were purchased from either Fisher Scientific (Pittsburgh, PA, USA), or Sigma–Aldrich (St Louis, MO, USA).

## Antibodies

Antibodies used were as follows: a mouse monoclonal anti-IR (α-IRβ) primary antibody (1:100; AHR0271; Invitrogen—France); a rabbit polyclonal antibody raised against the C-terminus of the rat glucose transporter type 4 (GLUT4) (1:100; Cat # 07-1404; Millipore, Temecula, CA, USA), or a mouse monoclonal anti-GLUT4 (1:100; Cat # ab35826, Abcam, Cambridge, MA, USA); FSU120, a rabbit polyclonal antiserum targeting 46 amino acids between the C-terminal and the sixth transmembrane domain of the voltage-dependent potassium channel Kv1.3 (1:500) (Velez et al., 2017); a rabbit anti-laminin (1:100; Sigma-Aldrich), and an anti-GFAP (1:100; Cat # G 9269, Sigma-Aldrich, Saint-Quentin Fallavier, France).

## Immunocytochemistry

Adult male rats were anesthetized in the fasted state (before 11:00 a.m.) using an intraperitoneal injection of ketamine (Imalgene, 80 mg/kg, MERIAL, Lyon, France) and xylazine (Rompun, 10 mg/kg, Bayer, Puteaux, France). Rats were killed by decapitation and then the aPCtx was quickly removed and immediately frozen in liquid nitrogen. Sections were prepared and immunolabeled as previously described with slight modification (Julliard and Hartmann 1998). Briefly, brain sections (17 μm) were incubated for 15 min (min) in BS at room temperature (23 °C) to reduce non-specific binding. Sections were incubated overnight at 4 °C in dark chambers using one or several of the following primary antisera dilutions in BS: α-IRβ (1:100), α-GLUT4 (1:100), α-Kv1.3 (1:500), α-laminin (1:100), or GFAP (1:100). The following day, sections were washed with BS, and then incubated for 1 h (h) at room temperature with one of the following species-specific secondary antibodies diluted in BS: antirabbit IgG, anti-mouse IgG, or anti-goat secondary antisera coupled with either Cy3 (1:200, Jackson Immunoresearch, West Grove, PA, USA), Alexa 488 (1:100, Life Technologies Thermofisher Scientific, Villebon sur Yvette, France), or Cy5 (1:100, Jackson Immunoresearch, West Grove, PA, USA). Sections were mounted using Vectashield mounting medium (Cat # H-1200, Vector Laboratories CliniSciences; Nanterre, France) containing 4,6-diamidino-2-phenylindole (DAPI) to visualize nuclei. Omission of primary antisera served as the control experiment. Sections were examined using a Zeiss Apotome

epifluorescence microscope (Axio Imager Z1 stand, Zeiss; Oberkochen, Germany), equipped with an Axiocam MRm camera and Axiovision software (Zeiss).

## Piriform cortex slice electrophysiology

**Slice preparation—**To examine glucose and insulin sensitivities, rats were anesthetized with isoflurane (Aerrane; Baxter, Deerfield, IL, USA) using the drop-method and were quickly decapitated. Following anesthesia, the dorsal and lateral portions of the skull between the bregma and the lambda suture were removed to expose the cortex. The brain was cut at the midline, and the aPCtx was quickly isolated from each hemisphere by cutting coronally between the anterior olfactory nucleus and the superior colliculus. The posterior side of the aPCtx was then quickly glued to a sectioning block with Superglue (Lowe's Home Improvement, USA). Dissection and slicing were conducted in oxygenated ($95\%O_2/5\%CO_2$), ice-cold ACSF solution. Coronal sections were made at a 400 μm thickness using a vibratome (Leica Model 1000 or VT1000s, Wetzlar, Germany), and were incubated in an interface (Krimer and Goldman-Rakic 1997) or Gibb's chamber (Gibb and Edwards 1994) at 32 °C for 30 min, then at room temperature for 1 h prior to recording.

**Electrophysiological recording—**aPCtx slices were visualized at 10x and 40x using an Axioskop 2FS Plus microscope (Carl Zeiss Microimaging, Inc., Thornwood, NY, USA) equipped with infrared detection capabilities (Dage MT1, CCD100). aPCtx slices were continuously perfused (1–2 ml/min, Ismatec, Cole Palmer, Vernon City, IL) with oxygenated ACSF solution using a Warner recording chamber (RC-26, Warner Instruments, Hamden, CT, USA). Current-clamp recordings were acquired using an Axopatch 200B amplifier (Axon Instruments, Molecular Devices, Sunnyvale, CA, USA) and the analog signal was low-pass filtered at 2 kHz and digitally sampled every 100 μs. The electrodes used were pulled from borosilicate glass (#1405002; Hilgenberg GmbH, Malsfeld, Germany) to yield resistances ranging from 4 to 7 MΩ. Within Layer II of the aPCtx, there are two major principal neurons that receive input from the OB: the superficial pyramidal (SP) cells and the semilunar (SL) cells that lack basal dendrites. In our study, we tried to target only the SP cells by navigating the patch pipette towards the deep half of Layer II (Layer IIb), and further identified this subclass of neurons based upon distinct morphology and biophysical properties (Suzuki and Bekkers 2006). After establishing a whole-cell configuration, cell health and integrity of the seal were monitored by resting potential (− 65 mV; not corrected for the liquid junction potential), input resistance (120 MΩ), and series resistance (< 20 MΩ) over time. Input resistance was obtained by applying a series of hyperpolarizing 50 pA current steps starting at −200 pA, every 1 s for 800 ms while clamping the membrane potential to – 50 mV so that the data could be statistically evaluated across cells. The perithreshold current was determined by incrementally injecting 800 ms long, 50 pA steps of current every 10 s, starting at – 50 pA. The current that consistently elicited a train of 5 or more action potentials (APs) was then re-injected for the remainder of the experiment to compare the effect of different glucose or insulin concentrations on AP frequency. Cells were stimulated with the perithreshold current for 800 ms at an interpulse interval of 10 s for glucose recordings and 20 s for insulin recordings. Insulin has been reported to have an effect on the electrical activity of MCs within 20 min of bath application (Fadool et al. 2000). Therefore, we prolonged the interpulse interval to prevent spike adaptation caused by

the intrinsic properties of SP. AP firing frequency and instantaneous AP frequency (IF) were calculated for each neuron. The IF of SP was calculated based on (Suzuki and Bekkers 2006) as $1/\Delta tn$ where $\Delta tn$ was the time interval between $AP_n$ and $AP_{n+1}$.

## Microinjections and behavioral testing

**Micro-surgery and cannula implantation—**Adult male rats ($n = 36$) were weighed and anesthetized using an intraperitoneal injection of ketamine/xylazine mixture (80/10 mg/Kg). The surgery performed was modified from (Julliard et al. 2007). Briefly, rats were restrained in a Stoelting stereotaxic apparatus (Ultra Precise Dual Lab Standard™, Wood Dale, IL, USA). The skull was exposed and 2 holes were drilled over the aPCtx. Two cannula guides (26 gauge, C315GA/SPC, Plastic One, San Diego, CA, USA) were implanted bilaterally at the following stereotaxic coordinates: AP – 3.7 mm from bregma, M/L + 2.7 and D/V – 5.6 mm from dura (Paxinos and Watson 2007; Fig. 1a). Surgical screws (743 1058, Phymep, Paris, France) were implanted between the bregma and the lambda on each side of the cerebral hemispheres (Fig. 1a) and were anchored to the skull and cannulae using dental cement (Phymep, Paris, France). Dummy cannulae (C315DC, Plastic One) were inserted into guide cannulae and remained there until injection time. Evans Blue was used to monitor the injection site and trace the approximate diffusion pattern of the injected substance (Fig. 1b).

**Whole body plethysmograph—**Behavioral testing was performed inside a whole-body, customized plethysmograph (EMKA technologies, Paris, France) previously described by Hegoburu et al. (2011). The plethysmograph was placed inside a custom-made, sound-attenuating chamber, and was connected to a custom-made olfactometer (CRNL customized, Lyon, France) that was programmed to pump non-odorized or 10% odorized air at a rate of 2 L/min (Fig. 2). A ventilation pump at the bottom drew air out at an equal rate to prevent interference with the sniffing signal. A differential pressure transducer measured the changes in air pressure between the animal chamber and a reference chamber thereby providing a measure of respiratory behavior in rodents. The signal was acquired at 1 kHz using an acquisition card (MC-1608FS, Measurement Computing, Norton, MA, USA USA). Animal's behavior was monitored using 2 infra-red video cameras placed at two opposite corners of the sound-attenuating cage.

Because no change in peripheral blood glucose and insulin has been observed upon injection of insulin into central olfactory areas (Aimé et al. 2012; Marks et al. 2009), no serum chemistry determinations were made across treatment groups following recovery from surgery. After the surgery, rats were allowed 7 days to recover, then they were gradually habituated to a 20 h/day food restriction schedule in which they had access to food from 11:00 a.m. to 3:00 p.m. only (Fig. 3a). Once the diet was set up, the sniffing behavior protocol was performed for 5 days: 4 days of acclimation followed by one day of discrimination test. The acclimation phase consisted of seven consecutive presentations of clean air (blank or Bl; Fig. 3b) for a total of 20 min. On the fifth day, olfactory discrimination was evaluated on fasted rats injected with either ACSF (control), glucose (10 mM), insulin (172 nM), or margatoxin (0.1 nM); all diluted in ACSF (Fig. 3a).

Discrimination was evaluated through a habituation/dishabituation paradigm, also called cross-habituation paradigm (Cleland et al. 2002; Fletcher and Wilson 2001), using three different pairs of odors. Each olfactory task required high-acuity discrimination because similar odorant pairs were tested using a context involving no reward associations. Using sniff measurements seems optimally suited to investigate habituation and discrimination tasks (Coronas-Samano et al. 2016). Because odor novelty was essential in our experimental procedure, the animals were never previously exposed to the three odor pairs and each animal was tested only once for each odor pair. The sniffing behavioral protocol consisted of two presentations of Bl, four successive trials corresponding to four presentations of odor A, and a fifth and last trial corresponding to the presentation of odor B. Odor presentations lasted for 10 s, and inter-trial intervals lasted for 3 min. Starting with clean air presentation allowed us to establish a control baseline of sniffing frequency that we defined as the steady state.

Following the steady state, the repetitive stimulation with odor A induced a progressive decrease in olfactory responsiveness called habituation. Finally, introduction of odor B in the chamber yielded two possible sniffing behaviors in the rats: (1) enhancement of the sniffing frequency showing that the rat had discriminated between odor A and odor B, or (2) a similar sniffing frequency between the 4th presentation of odor A and presentation of odor B that indicated that the rat did not discriminate between odor A and odor B.

**Odorants—**To observe the impact of metabolism on odorant discrimination, odor pairs were chosen based on the difficulty to discriminate between them. Odors with similar physicochemical properties (Rojas-Libano and Kay 2012) i.e., enantiomers, and odorants varying only by one carbon were selected and used alone or in a mixture. The following pairs of odorants were used at saturated vapor pressure (odor A vs. odor B): (1) rose oxide (−) (RO) vs. rose oxide (+) (RO), (2) a mixture of 70% limonene (+)/30% limonene (−) (L/L) vs. 70% limonene (−)/30% limonene (+) (L/L), and (3) an odorant, ethyl-hexanoate (E6) vs. a binary odorant mixture: ethyl-hexanoate 70%/ethyl-heptanoate 30% (E6/E7).

**Data acquisition and statistical analysis—**Electrophysiological data were analyzed using Clampfit 10.3 (Axon CNS), in combination with the analysis packages Origin 8.0 (MicroCal Software, Northampton, MA, USA) and Igor Pro 6.0.2 (Wavemetrics Inc., Portland, OR, USA) with the NeuroMatics 2.02 plugin (written by Jason Rothman). Baseline and treatment values were calculated from the mean of at least 10 consecutive traces. For statistical analyses, Prism 6.0 (GraphPad Software, Inc., La Jolla, CA, USA) was used to perform a paired *t*-test, a repeated measure (ANOVA), or a mixed ANOVA based on the number of groups and factors compared.

Respiratory signals were collected in a database called OpenElectrophy (Garcia and Fourcaud-Trocme 2009), and analyzed using a python script (Hegoburu et al. 2011). For each odor presentation (also called a trial), respiratory frequencies were sampled in 5 s bins starting from 5 s preceding odor onset (− 5 s) to 25 s after (25 s). The first two bins from − 5 s to 5 s ([− 5 s; + 5 s]) correspond to the baseline respiratory frequency during the steady state (before odor presentation) and the last four bins ranging from 5 s to 25 s ([+ 5 s; +25 s]) correspond to the sniffing frequency when odor A or odor B were presented.

The statistical analysis of the cross-habituation test compared respiratory frequencies between the three groups of rats injected with glucose, insulin or MgTx, and the control group (ACSF-injected) using a three-way repeated-measure ANOVA with micro-injections, bins, and trials as factors. A Student–Newman–Keuls (SNK) post-hoc test was used to complete the analysis when appropriate (Statview software) for multiple comparisons. Depending on the data set, statistical comparisons were performed using a non-parametric Mann–Whitney *U* test, or a paired Wilcoxon test.

All statistical tests were performed with a ≤ 0.05 confidence level; for the paired *t*-test; Wilcoxon or Student's *t* test (*$p < 0.05$, **$p < 0.01$, ***$p < 0.001$, and #$p < 0.0001$), and for the Mann–Whitney *U* test (φ$p < 0.05$, φφ$p < 0.01$, Δ$p < 0.0001$).

## Results

### Molecular markers of glucose and insulin sensing in the piriform cortex: immunohistochemistry of Kv1.3, GLUT4, and IR

The presence and possible interaction between Kv1.3, GLUT4, and IR in the aPCtx are not known. For an initial characterization of their expression in the aPCtx, we used an immunocytochemical approach to investigate distribution and overlap with GFAP in the three different layers of the aPCtx. Kv1.3 immunolabeling was detected in the LOT, in the outer part of Layer I (Layer Ia), and in Layers II and III (Figs. 4a, e, 5a, e). Kv1.3 labeling demonstrated a punctate expression in the LOT (Figs. 4a, e, 5a), which suggests that the channel is likely distributed on MCs/TCs axon terminals. Kv1.3 was more highly expressed in sublayer Ia than in the LOT, and it was absent in Layer Ib. In Layer II, Kv1.3 labeling was restricted to large DAPI-stained nuclei. This suggested that Kv1.3 may be expressed on the membrane of principal cells, but whether it was expressed in SP or semilunar cells could not be determined (Fig. 4e).

GLUT4 immunolabeling could be detected in the LOT, Layer II, and Layer III where Kv1.3 was also detected (Figs. 4b, d, f, h; 5b, d, f, h, j, l). GLUT4 labeling observed in the LOT was greater than that found for Kv1.3, especially in the deep part of the LOT where GLUT4 labeled neuronal processes. Doubled-labeling for GLUT4/ Kv1.3 in the LOT was punctiform where Kv1.3 labeling surrounded GLUT4-positive, large diameter (1–2 μm) processes (Fig. 5d, insert), which are hallmarks of MCs/TCs myelinated axons (Price and Sprich 1975). GLUT4, however, was not expressed in Layer Ia, at the intersection of the LOT and Layer I. This is the location where axons from the OB typically project to the aPCtx and lose their myelination (Price 1973). Comparing GLUT4 and Kv1.3 expression in Layers II and III indicated that punctiform Kv1.3 labeling was either expressed at the surface, the cytoplasm, or in the processes of principal neurons while GLUT4 was restricted around the nuclei (Figs. 4a, b, e, f, 5e, f, i, j).

IR was expressed in the LOT and in Layer II of the aPCtx (Figs. 4c, 5g, k). Kv1.3 is a substrate for insulin phosphorylation in the OB (Fadool et al. 2011) and it is well known that GLUT4 is an insulin-sensitive glucose transporter (see reviews: Leto and Saltiel 2012; Stockli et al. 2011). Therefore, we carried out triple labeling experiments to discern potential co-localization of Kv1.3, GLUT4, and IR proteins in aPCtx slices (Figs. 4d, 5h, l). There

were some neurons within Layers II and III that expressed Kv1.3, GLUT4, and IR (arrows, Fig. 4a–d). Our triple-labeling demonstrated that some neuronal soma expressed all three proteins (triple arrows, Fig. 5e–l), while other neurons co-expressed two of three proteins; either Kv1.3 and GLUT4 (arrow/arrowhead, Fig. 5e–l), Kv1.3 and IR (double arrowheads, Fig. 5e–l), or GLUT4 and IR (double arrows, Fig. 5e–l), and in very few neurons of Layer III only IR was found (arrow, Fig. 5i–l). In contrast to Layers II and III, there was no clear overlap of the three proteins in the LOT and Layer I.

Axon fibers of the LOT are mainly myelinated and connect with neuronal dendrites at the level of Layer Ia. Layer Ia is rich in synaptic connections, which strongly suggests the presence of astrocytes that can modulate synaptic transmission. Layer Ia can be recognized from Layer Ib based on the concentration of glial cells (Price 1973). To investigate this, we used an antibody directed against GFAP, the main component of the intermediate filaments in astrocytes (Bignami et al. 1972; Eng et al. 1971). GFAP labeling was found mainly in Layer Ia and to a lesser extent in the LOT, and in Layers Ib and II (Fig. 4g). GFAP was observed surrounding blood vessels and inside cellular processes (Fig. 5c). The preferential distribution of GFAP in Layer Ia was similar to the distribution of Kv1.3. GFAP was not co-localized with either Kv1.3 or GLUT4 (Fig. 4h). No specific immunolabeling was observed when the primary antibody was omitted (Data not shown).

## Glucose and insulin sensitivities of superficial pyramidal cells recorded in current clamp

**Glucose sensitivity—**SP cells typically responded to a depolarizing current step by firing two APs at high frequency during an initial burst followed by a tonic train of APs (Fig. 6a, d, g). Changing glucose concentrations in the bath was evaluated by measuring the IF of evoked APs.

Decreasing glucose concentration from 10 to 0.5 mM (Fig. 6a–c) or from 5 to 1 mM (Fig. 6d–f) clearly decreased the IF in most of the recorded cells with the main decrease happening within the initial burst. A total of 26 SP cells were sampled, 19 of which were glucose excited (Fig. 6a–f) and 7 were glucose insensitive (Fig. 6g–i). Regardless of the applied decrease in glucose concentration, a 2-way RM ANOVA demonstrated an effect for intervals [10 to 0.5 mM glucose, Fig. 6c, ($F_{(5,48)}$ = 18.65, $p < 0.0001$); 5 to 1 mM, Fig. 6f, ($F_{(5,60)}$ = 19.36, $p < 0.0001$)] and glucose concentration [10–0.5 mM glucose, Fig. 6c, ($F_{(1,48)}$ = 57.98, $p < 0.0001$); 5–1 mM, Fig. 6f, ($F_{(1,60)}$ = 142.5, $p < 0.0001$)]. There was a significant interaction between intervals and glucose concentration [10–0.5 mM glucose, Fig. 6c, ($F_{(6,48)}$ = 22.38, $p < 0.0001$); 5–1 mM, Fig. 6f, ($F_{(5,60)}$ = 28.93, $p < 0.0001$)]. A Bonferroni post-hoc testing IF for the different glucose concentrations revealed a strong decrease in the IF during the first interval for the two concentration changes, 10–0.5 mM and 5–1 mM glucose (Fig. 6c, f, $p < 0.0001$). The glucose-sensitive SP cells that were tested for a 10–0.5 mM concentration change (Fig. 6c) showed an initial IF (62.54 ± 5.53 Hz) that significantly decreased to 36.02 ± 5.89 Hz, $n = 8$ ($p < 0.0001$), whereas those that were tested for a 5–1 mM concentration change (Fig. 6f) showed an initial IF (49.8 ± 1.3 Hz) that significantly decreased to ± 0.8 Hz, $n = 11$ ($p < 0.0001$). Specifically, intervals 3, 4, 5, and 6 were significantly different when glucose concentration was lowered from 5 to 1 mM (Fig. 6f, $p < 0.05$; $p < 0.01$). A subpopulation of SP neurons (26.9%) was unresponsive when

glucose concentration decreased from 5 to 1 mM (Fig. 6g–i). These cells expressed a high initial IF of ± 2.0 Hz that remained unchanged at 1 mM glucose (78.2 ± 1.8 Hz, $n = 7$).

**Insulin sensitivity is dependent upon the glucose concentration—**Insulin application reduced the IF of SP cells for elevated glucose concentrations, i.e., 10 mM (Fig. 7a) and 5 mM (Fig. 7b). A two-way RM ANOVA demonstrated main effects for intervals [10 G + I, ($F_{(5,48)} = 75.51$, $p < 0.0001$); 5 G + I, ($F_{(9,60)} = 12.96$, $p < 0.0001$)] and insulin application [10 G + I, ($F_{(1,48)} = 61.12$, $p < 0.0001$); 5 G + I, ($F_{(1,60)} = 77.93$, $p < 0.0001$)]. An interaction between intervals and insulin application was observed [10 G + I, ($F_{(5,48)} = 3.718$, $p < 0.01$) ; 5 G + I, ($F_{(9,60)} = 3.801$, $p < 0.001$)]. A Bonferroni post-hoc test for insulin application revealed a strong decrease in the IF for the first interval ($p < 0.0001$) and a less pronounced effect for the following intervals ($p < 0.05$; $p < 0.01$). The insulin-sensitive SP cells (Fig. 7a) showed an initial IF (76.74 ± 4.83 Hz) that significantly decreased to 56.73 ± 5.81 $n = 9$ ($p < 0.0001$) and (Fig. 7b) showed an initial IF (86.16 ± 1.35 Hz) that significantly decreased to 48.39 ± 2.17 Hz $n = 7$ ($p < 0.0001$). Interestingly, insulin was ineffective in modulating IF at low glucose concentrations, i.e., 0.5 mM (Fig. 7c) the IF (42.45 ± 9.23 Hz) is maintained in the presence of insulin IF (38.79 ± 7.89 Hz) $n = 4$ (NS).

**Insulin sensitivity is dependent upon glucose metabolism—**To determine if insulin modulation metabolism-dependent, a series of experiments was performed in the presence of alloxan. Alloxan is a selective glucokinase inhibitor that blocks glucose entry into glycolysis (Dunn-Meynell et al. 2002). In the presence of 5 mM glucose (Fig. 8), insulin was first introduced and then alloxan was added. A representative raster plot (1 of 4 recordings) of the evoked AP firing frequency is shown in Fig. 8a. The raster reflects the basal firing frequency under a glucose steady-state (5 G) prior to the introduction of insulin (5 G + I) that causes suppression of AP firing and develops over the course of minutes. Alloxan is then applied (5 G + I + alloxan), which demonstrates a reversible block when washed with 5 G + I. The mean firing frequency at 45 min (25.42 ± 6.23 Hz, plus alloxan) compared with that at 20 min (17.04 ± 8.91 Hz, pre alloxan) is significantly different (paired $t$ test, $p < 0.002$, $n = 4$). The summary data for all 4 SP cells that were sequentially treated with the same solutions as in the raster plot are shown in Fig. 8b. A 2-way RM ANOVA revealed main effects for intervals ($F_{(9,90)} = 24.34$, $p < 0.0001$) and baths ($F_{(3,90)} = 77.56$, $p < 0.0001$). A Bonferroni post-hoc test for insulin application revealed a strong decrease in IF due to insulin for the first interval ($p < 0.0001$), which decreased from 90.67 ± 8.27 Hz to 59.14 ± 7.05 Hz and for the third and fourth intervals ($p < 0.05$). A Bonferroni post-hoc test for alloxan application, demonstrated that the inhibitor reversed the insulin-induced IF decrease for all interval. Together these data indicate alloxan blocks insulin effect and reverses the insulin-induced decrease suggesting that insulin effect depends on glucose metabolism.

**Insulin prevents the decrease glucose concentration effect—**We have shown that SP cells are sensitive to decreases in extracellular glucose concentration (Fig. 6c, f) and that modulation by insulin is dependent upon the initial extracellular glucose environment (Fig. 7). In the last step, we have tested the effect of glucose fluctuation (decrease or increase) when SP cells were maintained in a steady state insulin environment. In contrast to data

shown in Fig. 6c, in the presence of insulin, decreasing extracellular glucose from 10 to 0.5 mM failed to modulate the IF (Fig. 9a). However, if the original extracellular environment of the SP cells contained a trace amount of glucose (0.5 mM), then insulin failed to change IF and a switch to high glucose was effectively excitatory (Fig. 9b). For the high glucose environment (Fig. 9a), a two-way RM ANOVA showed main effects for intervals ($F_{(5,96)}$ = 104.6, $p < 0.0001$) and treatment ($F_{(2,96)}$ = 36.88, $p < 0.0001$). An interaction between intervals and treatment was observed ($F_{(10,96)}$ = 3.008, $p < 0.01$). The Bonferroni post-hoc test showed a decrease in IF across the addition of insulin treatment (10 G vs. 10 G + I; $p < 0.0001$; $p < 0.01$) but no significant difference following the switch of glucose treatment (10 G + I vs. 0.5 G + I). For the low glucose environment (Fig. 9b), a two-way RM ANOVA showed a main effect for intervals ($F_{(6,63)}$ = 6.449, $p < 0.001$) and treatment ($F_{(2,63)}$ = 7.702, $p < 0.001$). An interaction between intervals and treatment was observed ($F_{(12,63)}$ = 4.431, $p < 0.0001$). The Bonferroni post-hoc test showed no significant change in IF across the addition of insulin treatment (0.5 G vs. 0.5 G + I), but a retention of an increase in IF in response to a switch in glucose treatment (0.5 G + I vs. 10 G + I) ($p < 0.001$; $p < 0.01$). Altogether these data indicate that insulin blocks the SP response to glucose decrease (from 10 to 0.5 mM) but not to glucose increase (from 0.5 to 10 mM).

## aPCtx-dependent olfactory discrimination is influenced by metabolic signals in freely moving rats

**Insulin, glucose or Kv1.3 blocker effects on respiratory frequency during steady state:** Stress is reported to elevate resting respiratory rates in the absence of odor stimulation and also failed habituation to repeated odor stimuli (Carnevali et al. 2013). Albeit the fact that we incorporated control ACSF-injected rats into our experimental design, we also monitored steady-state respiratory rate prior to odor stimulation as a secondary control. Therefore, before the discrimination task, we compared steady-state respiratory frequency during the two first bins from − 5 s to 5 s ([− 5 s; + 5 s]) between injected vs. control animals (ACSF-injected) over five trials. In comparing four different animal cohorts (Fig. 10a, c, e, g), a threee-way RM ANOVA revealed no significant main effect of micro-injection, no interaction between micro-injection and bins, micro-injection and trials or micro-injection, bins and trials (Insulin RO vs. RO, $F_{(1,4,86)}$ = 1.106; Insulin L/L vs. L/L, $F_{(1,4,76)}$ = 0.116; Glucose E6 vs. E6/E7 $F_{(1,4,44)}$ = 0.385; MgTx E6/E7 $F_{(1,4,52)}$ = 0.022) for respiration rates prior to odor stimulation. Comparison of animals receiving a MgTx vs. control micro-injection revealed a significant difference for the last trial (Fig. 10g; Mann–Whitney test $p < 0.05$). Rat respiratory frequency during steady state was low (3.01 ± 0.11 Hz). These results indicate that insulin and glucose micro-injections did not affect the respiratory frequency, however, MgTx micro-injection lowered the frequency of respiratory steady state during the late stage of the recording (Fig. 10h).

**Insulin suppresses discrimination ability in difficult olfactory task:** Olfactory habituation and discrimination were evaluated by measuring the sniffing frequency from + 5 s to + 25 s during the first four trials (habituation) compared with that from + 5 s to + 25 s acquired during the fourth and fifth trails (OdA4 vs. OdB, discrimination). First, we examined the sniffing frequency of the rats exposed to a pair of enantiomers (RO vs. RO) following the microinjection of insulin (Fig. 10b). A three-way RM ANOVA showed main effects for trial

($F_{(3,3,189)}$ = 44.24, $p$ < 0.0001) and bins ($F_{(3,3,189)}$ = 5.99, $p$ < 0.005) but no effect for injection ($p$ = 0.98) during the habituation phase. Post-hoc test for trial, revealed a strong habituation to repeated presentation of RO represented by a significant decrease in sniffing frequency between odor presentation 1–3 (OdA1 > OdA2 > OdA3; OdA3 and OdA4 NS). Sniffing frequency fell from 8.26 ± 0.21 Hz to 3.47 ± 0.29 Hz for ACSF injection and from 7.83 ± 0.36 to 4.12 ± 0.39 Hz for insulin injection between the first and fourth presentations of RO (Fig. 10b).

For discrimination (comparison of the fourth presentation of RO to the fifth presentation of RO) the three-way RM ANOVA showed main effects of trial ($F_{(1,3,63)}$ = 35.75 $p$ < 0.0001) and bins ($F_{(1,3,63)}$=4.65 $p$ < 0.01) but no effect of insulin injection ($p$ = 0.22). The SNK post-hoc test for trial effect revealed that sniffing frequency recorded during OdA4 (4th presentation of RO; ACSF: 3.47 ± 0.29 Hz; insulin: 4.12 ± 0.39) was significantly lower than OdB (presentation of RO; ACSF: 5.45 ± 0.34 Hz; insulin: 6.07 ± 0.39 Hz), indicating that the two animal groups (ACSF and insulin injected) discriminated between the odor pair (paired Wilcoxon test $p$ < 0.0001; Fig. 10b). These collective results suggest that discriminating between RO and RO may be an easy task for fasted animals and that micro-injection of insulin into the piriform cortex of fasted animals does not modify olfactory discrimination.

Next, we elected to examine a more difficult discrimination task, the discrimination of mixtures of enantiomeric molecules. Here, fasted animals were presented four times with a mixture of 70% L/30% L followed by a fifth presentation where the proportions of the mixture were reversed (70% L/30% L). For habituation a three-way RM ANOVA performed on data included within recording interval [5 s-25 s], showed main effects for trial ($F_{(3,3,171)}$ = 37.23, $p$ < 0.0001) and bins ($F_{(3,3,171)}$ = 2.82, $p$ < 0.05) but no effect of insulin injection ($p$ = 0.33; Fig. 10d). The SNK post-hoc test revealed a significant decrease in sniffing frequency between the first and fourth odor presentation (OdA1 > OdA2 > OdA3 > OdA4—OdA1; ACSF: 8.92 ± 0.29 Hz; insulin: 8.53 ± 0.26 Hz—OdA2; ACSF: 6.19 ± 0.43 Hz; insulin: 5.69 ± 0.33 Hz—OdA3; ACSF: 4.96 ± 0.45 Hz; insulin: 4.84 ± 0.32 Hz—OdA4; ACSF: 4.39 ± 0.43 Hz; insulin: 3.64 ± 0.26 Hz).

For discrimination (comparison of fourth presentation of 70% L/30% L to the fifth presentation of 70% L/30% L) a three-way RM ANOVA demonstrated main effects for trial ($F_{(1,3,57)}$ = 5.93 $p$ < 0.05) and injection ($F_{(1,3,57)}$ = 7.28 $p$ < 0.05) but not for bins ($p$ = 0.28). The SNK post-hoc test for trial effect revealed that sniffing frequency recorded during OdA4 (fourth presentation of 70% L/30% L) was significantly lower than OdB (presentation of 70% L/30% L). In addition, the SNK post-hoc test for micro-injection indicated that sniffing frequency was significantly lower after insulin injection compared with that of ACSF. The sniffing frequency of control rats during OdA4 vs. OdB was significantly different ($p$ < 0.005; paired Wilcoxon test, ACSF—OdA4 = 4.39 ± 0.43 Hz; OdB = 6.16 ± 0.41; $n$ = 9; Fig. 10d), indicating that these two enantiomer mixtures were discriminated. Animals that were injected with insulin, however, did not exhibit this significant difference (insulin—OdA4 = 3.36 ± 0.26 Hz; OdB = 3.68 ± 0.33; $n$ = 12) indicating that this animal group had not discriminated the two enantiomeric mixtures. Data between ACSF vs. Insulin injected

rats for the fifth trial (novel odor presentation; L/L) were significantly different (Mann-Whitney U test $p < 0.0001$; Fig. 10d).

Altogether, our results indicate that using the easy olfactory task (i.e., discriminating between RO and RO), insulin injection did not affect odor discrimination, whereas using very difficult olfactory task (i.e., discriminating between enantiomeric molecule mixtures) fasted animals were able to discriminate enantiomeric mixtures. Insulin microinjection into the PCtx prevents this ability.

**Glucose suppresses discrimination, whereas Kv1.3 blocker alters habituation in difficult olfactory task:** In our final behavioral experiments, we examined olfactory performance of rats to a single odor vs. a binary odor mixture when microinjected with glucose (Fig. 10f) or a Kv1.3 ion channel blocker (Fig. 10h). Glucose- or MgTx-injected animals were asked to discriminate the odorant E6 from an odorant mixture containing E7: 70% E6/30% E7. For the habituation study, a three-way RM ANOVA demonstrated main effects for trial ($F_{(3,3,99)} = 21.33$, $p < 0.0001$, glucose and $F_{(3,3,117)} = 13.6$, $p < 0.0001$, MgTx), bins ($F_{(3,3,99)} = 7.21$, $p < 0.001$, glucose and $F_{(3,3,117)} = 5.14$, $p < 0.01$, MgTx), and injections ($F_{(3,3,117)} = 5.14$, $p < 0.05$, MgTx). An interaction between injection, trial and bins was observed for rats treated with glucose ($F_{(3,3,99)} = 2.68$, $p < 0.01$). In the corresponding SNK post-hoc test, rats exhibited a significant decrease in sniffing frequency between the first and fourth odor presentation (OdA1 > OdA2 > OdA3 > OdA4—OdA1; ACSF: 9.00 ± 0.32 Hz; glucose: 8.91 ± 0.34 Hz—OdA2; ACSF: 8.32 ± 0.44 Hz; glucose: 6.64 ± 0.39 Hz—OdA3; ACSF: 6.59 ± 0.48 Hz; glucose: 6.47 ± 0.48 Hz—OdA4; ACSF: 5.14 ± 0.58 Hz; glucose: 4.44 ± 0.48 Hz), revealing a strong habituation to repeated presentation of E6. For rats injected with MgTx, the post-hoc analysis (SNK) revealed a higher sniffing frequency during OdA1 compared to that in Od4 and as well as during OdA3 compared to OdA4 (OdA1; ACSF: 9.00 ± 0.32 Hz; MgTx: 8.88 ± 0.35 Hz—OdA2; ACSF: 8.32 ± 0.44 Hz; MgTx: 6.67 ± 0.48 Hz—OdA3; ACSF: 6.59 ± 0.48 Hz; MgTx: 4.72 ± 0.38 Hz—OdA4; ACSF: 5.14 ± 0.58 Hz; MgTx: 3.30 ± 34 Hz). The post-hoc test also indicated a lower sniffing frequency in MgTX-injected rats compared to that in ACSF-treated animals. These results indicate that both glucose and MgTx-treated rats exhibit a habituation process, however, the rate of habituation was the fasted in rats treated with MgTx (Fig. 10f–h).

For discrimination comparison of the fourth presentation of E6 to the fifth odor presentation (OdB = 70%E6/30% E7) a three-way ANOVA showed no main effects in glucose-treated rats for trial, bins, or injection ($F_{(1,3,33)} = 3.0$; 2.89 and 0.80). Nevertheless in control rats the sniffing frequency was significantly different ($p < 0.05$ Wilcoxon test) between OdA4 vs. OdB (ACSF—OdA4: 5.14 ± 0.58 Hz; OdB: 6.78 ± 0.43 Hz; $n = 8$) while in glucose injected rats the discrimination was lost ($p = 0.063$, Wilcoxon test, glucose—OdA4: 4.44 ± 0.48 Hz; OdB: 5.62 ± 0.58 Hz; $n = 6$; Fig. 10f). A three-way ANOVA for MgTx/ACSF injections showed main effects for trial ($F_{(1,3,39)} = 6.0$ $p < 0.05$), bins ($F_{(1,3,57)} = 8.36$ $p < 0.001$), and injection ($F_{(1,3,57)} = 5.21$ $p < 0.05$) (Fig. 10h). The SNK post-hoc test for trial effect revealed that sniffing frequency recorded during OdA4 (fourth presentation of E6) was significantly lower than OdB (presentation of E6 70%/E7 30%), indicating that this odor pair was discriminated. The SNK post-hoc test for injection effect revealed that sniffing frequency recorded after MgTx injection was significantly lower compared to ACSF injection. Unlike

what was observed with glucose injection, the sniffing frequency in MgTx-injected during OdA4 vs. OdB was significantly different ($p < 0.05$ and $p < 0.01$ respectively; ACSF—OdA4: 5.14 ± 0.58 Hz; OdB: 6.78 ± 0.43 Hz; $n = 8$; MgTx—OdA4: 3.30 ± 0.34 Hz; OdB: 5.32 ± 0.47 Hz; $n = 8$; paired Wilcoxon test, Fig. 10h). In summary, although discrimination between a pure odorant molecule vs. perceptively similar odorant mixtures is a difficult task, rats injected with glucose fail to discriminate, whereas those injected with MgTx increase habituation, but do not fail to discriminate.

## Discussion

Our study uses a multidisciplinary approach to show that the aPCtx detects an interplay between glucose and insulin. We immunochemically demonstrate that IR; the insulin-dependent glucose transporter, GLUT4; and the voltage-gated ion channel, Kv1.3; are present in the aPCtx and are co-localized in several cellular layers. Glucose and insulin modulate the excitability of SP cells of the aPCtx in vitro, and when injected in vivo, they decrease rat olfactory performance requiring high-acuity discrimination.

### Kv1.3, GLUT4, and IR are expressed in several layers of the aPCtx

We report the first immunochemical evidence for the expression of Kv1.3 channel in the aPCtx. Its detection is in corroboration with the earlier measurement of RNA expression of the channel using in situ hybridization (Kues and Wunder 1992). We show the first co-labeling of IR and GLUT4 in the aPCtx, which have been singly described (El Messari et al. 2002; Hill et al. 1986; Schulingkamp et al. 2000; Unger et al. 1989; Zhou et al. 2017). Our data indicate that the aPCtx expresses GLUT4, Kv1.3, and IR similar to that reported for other brain regions such as the OB, the cortex, and the hippocampus (Aime et al. 2012; Al Koborssy et al. 2014; Fadool and Levitan 1998; Fadool et al. 2000; Kobayashi et al. 1996; Kues and Wunder 1992; Marks et al. 1990; Unger et al. 1989). Having these three proteins co-localized would facilitate their functional interaction. It is known that Kv1.3 is a substrate for insulin phosphorylation in the N- and C-termini of the channel (Fadool and Levitan 1998; Fadool et al. 2000) and that block of the channel causes an upregulation of GLUT4 translocation for a transporter that is insulin dependent (Kovach et al. 2016; Li et al. 2006).

GLUT4, Kv1.3 and IR are located in the LOT, and Layers II and III of the aPCtx. Of the three explored signaling proteins, Kv1.3 was the only one detected in Layer I, and more precisely, in the upper part—Layer Ia. GFAP showed a similar distribution as that of Kv1.3 (LOT, Layers Ia, II and III) nevertheless GFAP was not co-localized with either Kv1.3 or GLUT4. Astrocytes classically express inward rectifying rather than delayed-rectifier type voltage-gated potassium channels, such as Kv1.3 (Djukic et al. 2007; Sibille et al. 2014), which may explain the lack of overlapping profiles that we saw between Kv1.3 and GFAP. The Layer Ia is rich in excitatory synaptic connections between axon terminals originating from the OB and from different olfactory cortices (the anterior olfactory nucleus, dorsal peduncular cortex, ventral tenia tecta, piriform cortex, olfactory tubercle, nucleus of the lateral olfactory tract, anterior cortical nucleus of the amygdala, periamygdaloid cortex, and lateral entorhinal cortex). This rich synaptic environment would explain the need for astrocytes to influence neuronal excitability, to provide nutrient support, and to clear excess

potassium in the extracellular compartment. In Layer Ia, the presence of Kv1.3 combined with the absence of GLUT4 might suggest that GLUT4 does not participate in synaptic transmission, unlike Kv1.3. Within Layers II and III, there were some neurons that expressed Kv1.3, GLUT4, and IR. Kv1.3 labeling appears punctiform compared with GLUT4, which might suggest a differential cellular expression.

### Superficial pyramidal cells express IR, GLUT4 and/or Kv1.3 and sense glucose and insulin via a metabolism-dependent pathway

At higher magnification in Layers II and III, triple labeling indicated that some SP cells expressed all three proteins—GLUT4, IR and Kv1.3—while others expressed only one or two of the three. The Kv1.3 labeling appeared punctiform consistently with membrane expression of Kv1.3 surrounding the cytoplasmic labelling of GLUT4. SP cells could be compared with MCs in the OB that have also been previously shown to co-express IR and GLUT4 (Aime et al. 2012; Al Koborssy et al. 2014), or GLUT4 and Kv1.3 mRNA (Kovach et al. 2016).

These proteins expressed in the aPCtx play a functional role that we have studied in current clamp.

### Pyramidal neurons are glucose and insulin-responsive

SP cells are responsive to glucose and insulin in a physiological range, which suggests that the co-localization of these proteins plays a functional role. Our electrophysiological data indicate that there are subpopulations of glucose-excited cells that insulin modulates the IF, and that insulin modulation requires glucose metabolism. To our knowledge, we are the first to report glucose-excited SP cells. Zhou et al. (2017) explored insulin modulation in the aPCtx at a steady-state glucose concentration where they found insulin increased excitation while decreasing inhibitory synaptic transmission to alter olfactory signaling. Here, we show that the effect of insulin depends on extracellular glucose concentration. Insulin decreases the IF of SP cells at high glucose concentration (5 to 10 mM) but prevents the reduction in IF when the extracellular glucose decreases below 5 mM. Insulin has no effect on the IF when the extracellular glucose is low (0.1–1 mM) but only promotes glucose-excitation.

Our data concerning glucose-dependent insulin modulation are consistent with studies reported in the hypothalamus. It has been demonstrated that insulin in the VMH suppresses the ability of neurons to sense high glucose concentration and that this insulin-induced inhibition was significantly attenuated in 2.5 and 0.1 mM glucose compared with that in 5 mM glucose (Cotero and Routh 2009). Suzuki and Bekkers (2006) have reported that the spike bursting pattern in SP cells during the first interval is due to a calcium channel. We, therefore, postulate that glucose and insulin sensing pathways involving IR, GLUT4, and Kv1.3 might have a common Ca channel as a downstream effector. Calcium is a common actor to glucose-sensing pancreatic cells and glucose-excited neurons in the VMH (Marty et al. 2007; Moriyama et al. 2004). Alternatively, in other brain regions, glucose-sensing neurons are governed by other ion channels such as the ATP-dependent K channels or chloride channels (Ainscow et al. 2002; Burdakov 2007; Burdakov and Lesage 2010). In the OB, the glucose-sensing ability of MCs is lost in Kv1.3−/− mice but the mechanism of

glucose modulation of this ATP- and Ca-insensitive channel is not known (Tucker et al. 2013).

The fact that alloxan prevents the insulin-induced decrease in IF and mean firing frequency indicates that there must be an ATP dependency or glucose metabolism component required for the modulation of both of these biophysical properties. How GLUT4, IR, and Kv1.3 are dependent upon ATP is incompletely known. Our GLUT4 immunocytochemical data suggest one putative connector between the observed insulin modulation and the need for glucose entry. Alloxan application that reversed the insulin-induced firing decrease would be anticipated to decrease ATP availability resulting from blocked glucose metabolism that was transported through GLUT4. In the hypothalamus, insulin modulation is known to signal via opening ATP-sensitive K channels (see for review: Wada et al. 2005), therefore, an ATP decrease could be suppressing insulin responses. In hypothalamic orexin neurons, a reduction in ATP or a reduction in energy background levels, promotes glucose sensitivity of orexin neurons (Venner et al. 2011). Certainly, a drop in ATP could open ATP-dependent potassium channels expressed in the PCtx to increase excitability and firing frequency (Karschin et al. 1997). Another connector in ATP dependency may reside at the level of mitochondria. In the OB, Kv1.3 is not only expressed in neuronal membranes but also in mitochondria where it regulates their size (Kovach et al. 2016). Certainly, the activity of mitochondrial Kv1.3 is linked to ROS and ATP production that regulate conductance and channel phosphorylation, respectively (Cayabyab et al. 2000; Fadool and Levitan 1998). Overall, the metabolism of glucose establishes the H gradient in mitochondria down the electron transport chain to produce ATP and the maintenance of this ionic environment is dependent upon the influx of K through mitochondrial Kv1.3. Future downstream mechanisms of glucose sensing and insulin modulation could explore not only the balance of energy availability and molecular targets but also modulation by other traditional sources of energy for neurons such as lactate (Venner et al. 2011).

## Insulin and glucose suppress discrimination ability while MgTx alters odor habituation

Because our electrophysiological data demonstrated that application of glucose and/or insulin functionally changed SP cells biophysics, we next explored whether changes in insulin or glucose availability could alter olfactory behaviors. The firing activity of select populations of neurons in the aPCtx is known to be modified during different components of odor discrimination tasks, including odor sampling, odor habituation, and response generation (Schoenbaum and Eichenbaum 1995; Wilson 2000). Our behavioral study showed that micro-injections of insulin, glucose, or MgTx in the aPCtx affected sniffing frequency mainly during discrimination and habituation tasks in a drug-dependent manner. During respiration, several parameters can be collected including amplitude and waveform of inhalation/exhalation (Youngentob 2005). Associating habituation/cross-habituation paradigm to respiration measurement using a plethysmograph system, we decided to focus our analysis on sniffing frequency, a major indicator of the relationship between sniffing and olfactory processing (Bathellier et al. 2008; Macrides et al. 1982; Verhagen et al. 2007; Wachowiak and Shipley 2006).

Regardless of the testing paradigm, presentation of the first odor elicited an increase in the sniffing frequency. This result indicates that micro-injections of glucose, insulin, or MgTx into the aPCtx did not affect sampling or animal interest to the novel odor. This is also in accordance with a number of previous studies performed in rodents exposed to a novel olfactory cue (Kepecs et al. 2007; Macrides et al. 1982; Welker 1964; Wesson et al. 2008; Youngentob et al. 1987). In fact, even age-related pathologies known to induce olfactory deficits do not affect sniffing patterns induced by exposure to novel odors (Wesson et al. 2011). Whether in physiological or pathological contexts, the sniffing frequency pattern for a novel odor is stereotyped and highly stable. This response profile is independent of olfactory perception changes, as well as of integration processing of olfactory information occurring in the aPCtx.

Repeated presentation of odor A decreased the sniffing frequency. This result indicates that rats have perceptive habituation to an odor and can adapt to environmental stimuli (Rankin et al. 2009). Insulin or glucose injected in the aPCtx did not affect habituation while MgTx induced a faster olfactory habituation. The MgTx effect on habituation could be mediated through the closure of Kv1.3 channels located in the superficial layers (LOT, Layer Ia) of the aPCtx. Indeed, it has been demonstrated that odor habituation for short odor exposures is associated with depression of synapses between MCs and PCs located in Layer Ia, see for review (Wilson 2009a). Our results suggest that the location of Kv1.3 in superficial layers could permit its participation in odor habituation driven by the aPCtx. Interestingly, Kv1.3 is thereby a key factor in olfactory processing—both for olfactory detection in the OB (Fadool et al. 2004), and as reported now for olfactory habituation in the aPCtx. In the aPCtx, further studies are needed to decipher the detailed molecular mechanisms involving Kv1.3. Indeed, we have shown that Kv1.3, GLUT4 and IR could be present in the same neurons and moreover, it has been reported that like in OB, these channels would be a key target for insulin's effect on SP (Zhou et al. 2017).

Presentation of the novel odor, or odor B, allows exploration of rat discrimination ability using a cross habituation paradigm. Micro-injections of insulin or glucose in the PCtx affected sniffing frequency during odor discrimination when using highly difficult olfactory tasks. These behavioral results are consistent with our found decrease in IF observed after insulin application and with previous results showing that the aPCtx is a critical site for discrimination and/or pattern separation. This allows the perceptual discrimination for very similar odor mixtures (Chapuis and Wilson 2011; Cohen-Matsliah et al. 2009; De Rosa and Hasselmo 2000; Haberly 2001; Staubli et al. 1987; Wilson 2009b; Wilson and Stevenson 2003). The present study suggests that metabolic signals such as insulin and glucose could act directly on the aPCtx network to modulate discrimination abilities. The aPCtx appears to be a key center of the discrimination process where sexual hormones (Wesson et al. 2006), neurotransmitters (see for review: Linster and Hasselmo 2001), and now metabolic molecules adapt discrimination abilities with physiological context. The ability to focally delete the contribution of insulin, glucose, and Kv1.3 signaling pathways in SP cells using a combination of pharmacological and genetic methods could be explored in the future to pinpoint the functional tie between metabolic sensing in the aPCtx and behavioral output. Knowing that changes in olfactory sensory neuron abundance (Riera et al. 2017) in the epithelium and changes in MC excitability in the OB (Fadool et al. 2004) both generate

changes in metabolism, is strong impetuous for exploring metabolic-based signaling in the next higher projection of olfactory information, the PCtx.

Combining functional data with our immunocytochemical and behavioral results, we conclude that glucose and insulin act both separately and in concert on the aPCtx network to influence olfactory discrimination. It is well documented that both insulin and glucose are crucial key components of memory processes (see for review: McNay and Cotero 2010; McNay and Recknagel 2011) and it has been demonstrated that GLUT4 present at hippocampal nerve terminals is mobilized by neuronal activity to support the energetic demands of firing synapses (Ashrafi et al. 2017). Similar to the hippocampus (Pearson-Leary and McNay 2016), we hypothesize that in the aPCtx, glucose uptake mediated through GLUT4 and insulin action, could fine-tune olfactory discrimination tasks. Discrimination is crucial to induce differential responses to stimuli according to their significance. In natural environments, animals face complex olfactory scents. Animals have to recognize and discriminate vital odors in odor backgrounds. Influence of metabolic signals on discrimination would have an obvious eco-ethological role by modulating the relevance of food odors related to palatability or edibility. Future studies investigating the driven behavioral responses induced by odor-orienting in rats should provide a better understanding of how these behaviors could be altered during metabolic pathologies such as obesity or diabetes. It will be of interest to investigate the effect of metabolic signals on habituation and discrimination to food odors vs. odors with other type of biological relevance.

## Acknowledgements

We would like to thank Ounsa Ben Hellal, Wesley Joshua Earl, and Abigail Thomas for routine technical assistance and rat husbandry.

**Funding** This work was supported by the Centre National de la Recherche Scientifique, University Lyon 1, the Laboratoire d'Excellence Cortex (ANR-11-LABX-0042), and the National Institutes of Health (NIH) R01 DC013080 from the National Institutes of Deafness and Communication Disorders (NIDCD). The collaboration was supported by a PALSE grant (Programme Avenir Lyon Saint-Etienne) from the University of Lyon 1; the Robert B. Short Zoology Scholarship, the Brenda Weems Bennison Endowment, and the Pasquale Graziadei Endowment Fund from The Florida State University.

## References

Aime P, Duchamp-Viret P, Chaput MA, Savigner A, Mahfouz M, Julliard AK (2007) Fasting increases and satiation decreases olfactory detection for a neutral odor in rats. Behav Brain Res 179(2):258–264. 10.1016/j.bbr.2007.02.012 [PubMed: 17367877]

Aime P, Hegoburu C, Jaillard T, Degletagne C, Garcia S, Messaoudi B, Thevenet M, Lorsignol A, Duchamp C, Mouly AM, Julliard AK (2012) A physiological increase of insulin in the olfactory bulb decreases detection of a learned aversive odor and abolishes food odor-induced sniffing behavior in rats. PLoS One 7(12):e51227 10.1371/journal.pone.0051227 [PubMed: 23251461]

Aime P, Palouzier-Paulignan B, Salem R, Al Koborssy D, Garcia S, Duchamp C, Romestaing C, Julliard AK (2014) Modulation of olfactory sensitivity and glucose-sensing by the feeding state in obese Zucker rats. Front Behav Neurosci 8:326 10.3389/fnbeh.2014.00326 [PubMed: 25278856]

Ainscow EK, Mirshamsi S, Tang T, Ashford ML, Rutter GA (2002) Dynamic imaging of free cytosolic ATP concentration during fuel sensing by rat hypothalamic neurones: evidence for ATP-independent control of ATP-sensitive K(+) channels. J Physiol 544(Pt 2):429–445 [PubMed: 12381816]

Al Koborssy D, Palouzier-Paulignan B, Salem R, Thevenet M, Romestaing C, Julliard AK (2014) Cellular and molecular cues of glucose sensing in the rat olfactory bulb. Front Neurosci 8:333 10.3389/fnins.2014.00333 [PubMed: 25400540]

Anand BK, Chhina GS, Sharma KN, Dua S, Singh B (1964) Activity of single neurons in the hypothalamic feeding centers: effect of glucose. Am J Physiol 207:1146–1154 [PubMed: 14237464]

Ashrafi G, Wu Z, Farrell RJ, Ryan TA (2017) GLUT4 mobilization supports energetic demands of active synapses. Neuron 93(3):606–615 e603 10.1016/j.neuron.2016.12.020 [PubMed: 28111082]

Balfour RH, Hansen AM, Trapp S (2006) Neuronal responses to transient hypoglycaemia in the dorsal vagal complex of the rat brainstem. J Physiol 570(Pt 3):469–484. 10.1113/jphysiol.2005.098822 [PubMed: 16284073]

Banks WA, Kastin AJ, Pan W (1999) Uptake and degradation of blood-borne insulin by the olfactory bulb. Peptides 20(3):373–378 [PubMed: 10447096]

Barnes DC, Hofacer RD, Zaman AR, Rennaker RL, Wilson DA (2008) Olfactory perceptual stability and discrimination. Nat Neurosci 11(12):1378–1380. 10.1038/nn.2217 [PubMed: 18978781]

Baskin DG, Porte D, Guest K, Dorsa DM (1983) Regional concentrations of insulin in the rat brain. Endocrinology 112(3):898–903 [PubMed: 6337049]

Bathellier B, Buhl DL, Accolla R, Carleton A (2008) Dynamic ensemble odor coding in the mammalian olfactory bulb: sensory information at different timescales. Neuron 57(4):586–598. 10.1016/j.neuron.2008.02.011 [PubMed: 18304487]

Bignami A, Eng LF, Dahl D, Uyeda CT (1972) Localization of the glial fibrillary acidic protein in astrocytes by immunofluorescence. Brain Res 43(2):429–435 [PubMed: 4559710]

Blevins JE, Truong BG, Gietzen DW (2004) NMDA receptor function within the anterior piriform cortex and lateral hypothalamus in rats on the control of intake of amino acid-deficient diets. Brain Res 1019(1–2):124–133. 10.1016/j.brainres.2004.05.089 [PubMed: 15306246]

Burdakov D (2007) K + channels stimulated by glucose: a new energy-sensing pathway. Pflugers Arch 454(1):19–27. 10.1007/s00424-006-0189-8 [PubMed: 17206449]

Burdakov D, Lesage F (2010) Glucose-induced inhibition: how many ionic mechanisms? Acta Physiol (Oxf) 198(3):295–301. 10.1111/j.1748-1716.2009.02005.x [PubMed: 19473131]

Carnevali L, Sgoifo A, Trombini M, Landgraf R, Neumann ID, Nalivaiko E (2013) Different patterns of respiration in rat lines selectively bred for high or low anxiety. PLoS One 8(5):e64519 10.1371/journal.pone.0064519 [PubMed: 23691240]

Cayabyab FS, Khanna R, Jones OT, Schlichter LC (2000) Suppression of the rat microglia Kv1.3 current by src-family tyrosine kinases and oxygen/glucose deprivation. Eur J Neurosci 12(6):1949–1960 [PubMed: 10886336]

Chapuis J, Wilson DA (2011) Bidirectional plasticity of cortical pattern recognition and behavioral sensory acuity. Nat Neurosci 15(1):155–161. 10.1038/nn.2966 [PubMed: 22101640]

Cleland TA, Morse A, Yue EL, Linster C (2002) Behavioral models of odor similarity. Behav Neurosci 116(2):222–231 [PubMed: 11996308]

Cohen-Matsliah SI, Rosenblum K, Barkai E (2009) Olfactory-learning abilities are correlated with the rate by which intrinsic neuronal excitability is modulated in the piriform cortex. Eur J Neurosci 30(7):1339–1348. 10.1111/j.1460-9568.2009.06894.x [PubMed: 19769594]

Colley BS, Biju KC, Visegrady A, Campbell S, Fadool DA (2007) Neurotrophin B receptor kinase increases Kv subfamily member 1.3 (Kv1.3) ion channel half-life and surface expression. Neuroscience 144(2):531–546. 10.1016/j.neuroscience.2006.09.055 [PubMed: 17101229]

Coronas-Samano G, Ivanova AV, Verhagen JV (2016) The habituation/cross-habituation test revisited: guidance from sniffing and video tracking. Neural Plast 2016:9131284 10.1155/2016/9131284 [PubMed: 27516910]

Cotero VE, Routh VH (2009) Insulin blunts the response of glucose-excited neurons in the ventrolateral-ventromedial hypothalamic nucleus to decreased glucose. Am J Physiol Endocrinol Metab 296(5):E1101–E1109. 10.1152/ajpendo.90932.2008 [PubMed: 19223652]

De Rosa E, Hasselmo ME (2000) Muscarinic cholinergic neuromodulation reduces proactive interference between stored odor memories during associative learning in rats. Behav Neurosci 114(1):32–41 [PubMed: 10718260]

Dematte ML, Endrizzi I, Biasioli F, Corollaro ML, Pojer N, Zampini M, Aprea E, Gasperi F (2013) Food neophobia and its relation with olfactory ability in common odour identification. Appetite 68:112–117. 10.1016/j.appet.2013.04.021 [PubMed: 23632036]

Djukic B, Casper KB, Philpot BD, Chin LS, McCarthy KD (2007) Conditional knock-out of Kir4.1 leads to glial membrane depolarization, inhibition of potassium and glutamate uptake, and enhanced short-term synaptic potentiation. J Neurosci 27(42):11354–11365. 10.1523/JNEUROSCI.0723-07.2007 [PubMed: 17942730]

Dunn-Meynell AA, Routh VH, Kang L, Gaspers L, Levin BE (2002) Glucokinase is the likely mediator of glucosensing in both glucose-excited and glucose-inhibited central neurons. Diabetes 51(7):2056–2065 [PubMed: 12086933]

Ekstrand JJ, Domroese ME, Johnson DM, Feig SL, Knodel SM, Behan M, Haberly LB (2001) A new subdivision of anterior piriform cortex and associated deep nucleus with novel features of interest for olfaction and epilepsy. J Comp Neurol 434(3):289–307 [PubMed: 11331530]

El Messari S, Ait-Ikhlef A, Ambroise DH, Penicaud L, Arluison M (2002) Expression of insulin-responsive glucose transporter GLUT4 mRNA in the rat brain and spinal cord: an in situ hybridization study. J Chem Neuroanat 24(4):225–242. (S0891061802000583 [pii]) [PubMed: 12406499]

Eng LF, Vanderhaeghen JJ, Bignami A, Gerstl B (1971) An acidic protein isolated from fibrous astrocytes. Brain Res 28(2):351–354 [PubMed: 5113526]

Fadool DA, Levitan IB (1998) Modulation of olfactory bulb neuron potassium current by tyrosine phosphorylation. J Neurosci 18(16):6126–6137 [PubMed: 9698307]

Fadool DA, Tucker K, Phillips JJ, Simmen JA (2000) Brain insulin receptor causes activity-dependent current suppression in the olfactory bulb through multiple phosphorylation of Kv1.3. J Neurophysiol 83(4):2332–2348 [PubMed: 10758137]

Fadool DA, Tucker K, Perkins R, Fasciani G, Thompson RN, Parsons AD, Overton JM, Koni PA, Flavell RA, Kaczmarek LK (2004) Kv1.3 channel gene-targeted deletion produces “Super-Smeller Mice” with altered glomeruli, interacting scaffolding proteins, and biophysics. Neuron 41(3):389–404. (S0896627303008444 [pii]) [PubMed: 14766178]

Fadool DA, Tucker K, Pedarzani P (2011) Mitral cells of the olfactory bulb perform metabolic sensing and are disrupted by obesity at the level of the Kv1.3 ion channel. PLoS One 6(9):e24921 10.1371/journal.pone.0024921 [PubMed: 21966386]

Fletcher M, Wilson DA (2001) Ontogeny of odor discrimination: a method to assess novel odor discrimination in neonatal rats. Physiol Behav 74(4–5):589–593 [PubMed: 11790419]

Franks KM, Isaacson JS (2005) Synapse-specific downregulation of NMDA receptors by early experience: a critical period for plasticity of sensory input to olfactory cortex. Neuron 47(1):101–114. 10.1016/j.neuron.2005.05.024 [PubMed: 15996551]

Garcia S, Fourcaud-Trocme N (2009) OpenElectrophy: an electrophysiological data- and analysis-sharing framework. Front Neuroinform 3:14 10.3389/neuro.11.014.2009 [PubMed: 19521545]

Gibb AJ, Edwards FA (1994) Patch clamp recording from cells in sliced tissues. In: Microelectrode Techniques. The Plymouth Workshop Handbook, Cambridge

Grundy D (2015) Principles and standards for reporting animal experiments in The Journal of Physiology and Experimental Physiology. J Physiol 593(12):2547–2549. 10.1113/JP270818 [PubMed: 26095019]

Haberly LB (1983) Structure of the piriform cortex of the opossum. I. Description of neuron types with Golgi methods. J Comp Neurol 213(2):163–187. 10.1002/cne.902130205 [PubMed: 6841668]

Haberly LB (2001) Parallel-distributed processing in olfactory cortex: new insights from morphological and physiological analysis of neuronal circuitry. Chem Senses 26(5):551–576 [PubMed: 11418502]

Hegoburu C, Shionoya K, Garcia S, Messaoudi B, Thevenet M, Mouly AM (2011) The RUB cage: respiration–ultrasonic vocalizations–behavior acquisition setup for assessing emotional memory in rats. Front Behav Neurosci 5:25 10.3389/fnbeh.2011.00025 [PubMed: 21637320]

Hill JM, Lesniak MA, Pert CB, Roth J (1986) Autoradiographic localization of insulin receptors in rat brain: prominence in olfactory and limbic areas. Neuroscience 17(4):1127–1138 [PubMed: 3520377]

Julliard AK, Hartmann DJ (1998) Spatiotemporal patterns of expression of extracellular matrix molecules in the developing and adult rat olfactory system. Neuroscience 84(4):1135–1150 [PubMed: 9578401]

Julliard A, Chaput M, Apelbaum A, Aime P, Mahfouz M, Duchamp-Viret P (2007) Changes in rat olfactory detection performance induced by orexin and leptin mimicking fasting and satiation. Behav Brain Res 183(2):123–129 [PubMed: 17624453]

Julliard AK, Al Koborssy D, Fadool DA, Palouzier-Paulignan B (2017) Nutrient sensing: another chemosensitivity of the olfactory system. Front Physiol 8:468 10.3389/fphys.2017.00468 [PubMed: 28747887]

Kapur A, Lytton WW, Ketchum KL, Haberly LB (1997) Regulation of the NMDA component of EPSPs by different components of postsynaptic GABAergic inhibition: computer simulation analysis in piriform cortex. J Neurophysiol 78(5):2546–2559. 10.1152/jn.1997.78.5.2546 [PubMed: 9356404]

Karschin C, Ecke C, Ashcroft FM, Karschin A (1997) Overlapping distribution of K(ATP) channel-forming Kir6.2 subunit and the sulfonylurea receptor SUR1 in rodent brain. FEBS Lett 401(1):59–64 [PubMed: 9003806]

Kaul L, Berdanier CD (1975) Effect of meal-feeding on the daily variations of insulin, glucose, and NADP-linked dehydrogenases in rats. J Nutr 105(9):1132–1140 [PubMed: 1159528]

Kepecs A, Uchida N, Mainen ZF (2007) Rapid and precise control of sniffing during olfactory discrimination in rats. J Neurophysiol 98(1):205–213. 10.1152/jn.00071.2007 [PubMed: 17460109]

Kobayashi M, Nikami H, Morimatsu M, Saito M (1996) Expression and localization of insulin-regulatable glucose transporter (GLUT4) in rat brain. Neurosci Lett 213(2):103–106 [PubMed: 8858619]

Kovach CP, Al Koborssy D, Huang Z, Chelette BM, Fadool JM, Fadool DA (2016) Mitochondrial ultrastructure and glucose signaling pathways attributed to the Kv1.3 Ion channel. Front Physiol 7:178 10.3389/fphys.2016.00178 [PubMed: 27242550]

Krimer LS, Goldman-Rakic PS (1997) An interface holding chamber for anatomical and physiological studies of living brain slices. J Neurosci Methods 75(1):55–58 [PubMed: 9262144]

Kuczewski N, Fourcaud-Trocme N, Savigner A, Thevenet M, Aime P, Garcia S, Duchamp-Viret P, Palouzier-Paulignan B (2014) Insulin modulates network activity in olfactory bulb slices: impact on odour processing. J Physiol 592(13):2751–2769. 10.1113/jphysiol.2013.269639 [PubMed: 24710056]

Kues WA, Wunder F (1992) Heterogeneous expression patterns of mammalian potassium channel genes in developing and adult rat brain. Eur J Neurosci 4(12):1296–1308 [PubMed: 12106393]

Lacroix MC, Caillol M, Durieux D, Monnerie R, Grebert D, Pellerin L, Repond C, Tolle V, Zizzari P, Baly C (2015) Long-lasting metabolic imbalance related to obesity alters olfactory tissue homeostasis and impairs olfactory-driven behaviors. Chem Senses 40(8):537–556. 10.1093/chemse/bjv039 [PubMed: 26209545]

Leto D, Saltiel AR (2012) Regulation of glucose transport by insulin: traffic control of GLUT4. Nat Rev Mol Cell Biol 13(6):383–396. 10.1038/nrm3351 [PubMed: 22617471]

Li Y, Wang P, Xu J, Desir GV (2006) Voltage-gated potassium channel Kv1.3 regulates GLUT4 trafficking to the plasma membrane via a Ca2+-dependent mechanism. Am J Physiol Cell Physiol 290(2):C345–C351. 10.1152/ajpce11.00091.2005 [PubMed: 16403947]

Linster C, Hasselmo ME (2001) Neuromodulation and the functional dynamics of piriform cortex. Chem Senses 26(5):585–594 [PubMed: 11418504]

Macrides F, Eichenbaum HB, Forbes WB (1982) Temporal relationship between sniffing and the limbic theta rhythm during odor discrimination reversal learning. J Neurosci 2(12):1705–1717 [PubMed: 7143047]

Marks JL, Porte D, Stahl WL, Baskin DG (1990) Localization of insulin receptor mRNA in rat brain by in situ hybridization. Endocrinology 127(6):3234–3236. 10.1210/endo-127-6-3234 [PubMed: 2249648]

Marks DR, Tucker K, Cavallin MA, Mast TG, Fadool DA (2009) Awake intranasal insulin delivery modifies protein complexes and alters memory, anxiety, and olfactory behaviors. J Neurosci 29(20):6734–6751. 10.1523/JNEUROSCI.1350-09.2009 [PubMed: 19458242]

Marty N, Dallaporta M, Thorens B (2007) Brain glucose sensing, counterregulation, and energy homeostasis. Physiology (Bethesda) 22:241–251. 10.1152/physiol.00010.2007 [PubMed: 17699877]

McNay EC, Cotero VE (2010) Mini-review: impact of recurrent hypoglycemia on cognitive and brain function. Physiol Behav 100(3):234–238. 10.1016/j.physbeh.2010.01.004 [PubMed: 20096711]

McNay EC, Recknagel AK (2011) Brain insulin signaling: a key component of cognitive processes and a potential basis for cognitive impairment in type 2 diabetes. Neurobiol Learn Mem 96(3):432–442. 10.1016/j.nlm.2011.08.005 [PubMed: 21907815]

Moriyama R, Tsukamura H, Kinoshita M, Okazaki H, Kato Y, Maeda K (2004) In vitro increase in intracellular calcium concentrations induced by low or high extracellular glucose levels in ependymocytes and serotonergic neurons of the rat lower brainstem. Endocrinology 145(5):2507–2515. 10.1210/en.2003-1191 [PubMed: 14962992]

Oomura Y, Ono T, Ooyama H, Wayner MJ (1969) Glucose and osmosensitive neurones of the rat hypothalamus. Nature 222(5190):282–284 [PubMed: 5778398]

Palouzier-Paulignan B, Lacroix MC, Aime P, Baly C, Caillol M, Congar P, Julliard AK, Tucker K, Fadool DA (2012) Olfaction under metabolic influences. Chem Senses 37(9):769–797. 10.1093/chemse/bjs059 [PubMed: 22832483]

Paxinos G, Watson C (2007) the rat brain in stereotaxic coordinates In: 123Library. 6 edn Academic Press

Pearson-Leary J, McNay EC (2016) Novel roles for the insulin-regulated glucose transporter-4 in hippocampally dependent memory. J Neurosci 36(47):11851–11864. 10.1523/JNEUROSCI.1700-16.2016 [PubMed: 27881773]

Price JL (1973) An autoradiographic study of complementary laminar patterns of termination of afferent fibers to the olfactory cortex. J Comp Neurol 150(1):87–108. 10.1002/cne.901500105 [PubMed: 4722147]

Price JL, Sprich WW (1975) Observations on the lateral olfactory tract of the rat. J Comp Neurol 162(3):321–336. 10.1002/cne.901620304 [PubMed: 1150925]

Ranade S, Hangya B, Kepecs A (2013) Multiple modes of phase locking between sniffing and whisking during active exploration. J Neurosci 33(19):8250–8256. 10.1523/JNEUROSCI.3874-12.2013 [PubMed: 23658164]

Rankin CH, Abrams T, Barry RJ, Bhatnagar S, Clayton DF, Colombo J, Coppola G, Geyer MA, Glanzman DL, Marsland S, McSweeney FK, Wilson DA, Wu CF, Thompson RF (2009) Habituation revisited: an updated and revised description of the behavioral characteristics of habituation. Neurobiol Learn Mem 92(2):135–138. 10.1016/j.nlm.2008.09.012 [PubMed: 18854219]

Ren X, Zhou L, Terwilliger R, Newton SS, de Araujo IE (2009) Sweet taste signaling functions as a hypothalamic glucose sensor. Front Integr Neurosci 3:12 10.3389/neuro.07.012.2009 [PubMed: 19587847]

Riera CE, Tsaousidou E, Halloran J, Follett P, Hahn O, Pereira MMA, Ruud LE, Alber J, Tharp K, Anderson CM, Bronneke H, Hampel B, Filho CDM, Stahl A, Bruning JC, Dillin A (2017) The Sense of Smell Impacts Metabolic Health and Obesity. Cell Metab 26(1):198–211 e195 10.1016/j.cmet.2017.06.015 [PubMed: 28683287]

Rojas-Libano D, Kay LM (2012) Interplay between sniffing and odorant sorptive properties in the rat. J Neurosci 32(44):15577–15589. 10.1523/JNEUROSCI.1464-12.2012 [PubMed: 23115193]

Rojas-Libano D, Frederick DE, Egana JI, Kay LM (2014) The olfactory bulb theta rhythm follows all frequencies of diaphragmatic respiration in the freely behaving rat. Front Behav Neurosci 8:214 10.3389/fnbeh.2014.00214 [PubMed: 24966821]

Rudell JB, Rechs AJ, Kelman TJ, Ross-Inta CM, Hao S, Gietzen DW (2011) The anterior piriform cortex is sufficient for detecting depletion of an indispensable amino acid, showing independent cortical sensory function. J Neurosci 31(5):1583–1590. 10.1523/JNEUROSCI.4934-10.2011 [PubMed: 21289166]

Sachse S, Beshel J (2016) The good, the bad, and the hungry: how the central brain codes odor valence to facilitate food approach in *Drosophila*. Curr Opin Neurobiol 40:53–58. 10.1016/j.conb.2016.06.012 [PubMed: 27393869]

Schoenbaum G, Eichenbaum H (1995) Information coding in the rodent prefrontal cortex. I. Single-neuron activity in orbitofrontal cortex compared with that in pyriform cortex. J Neurophysiol 74(2):733–750. 10.1152/jn.1995.74.2.733 [PubMed: 7472378]

Schulingkamp RJ, Pagano TC, Hung D, Raffa RB (2000) Insulin receptors and insulin action in the brain: review and clinical implications. Neurosci Biobehav Rev 24(8):855–872 [PubMed: 11118610]

Shepherd GM (2004) The synaptic organization of the brain, 5th edn Oxford University Press, Oxford; New York

Sibille J, Pannasch U, Rouach N (2014) Astroglial potassium clearance contributes to short-term plasticity of synaptically evoked currents at the tripartite synapse. J Physiol 592(1):87–102. 10.1113/jphysiol.2013.261735 [PubMed: 24081156]

Sitren HS, Stevenson NR (1978) The effects of meal-feeding at different times of the day on daily changes in serum insulin, gastrin and liver enzymes in the rat. J Nutr 108(9):1393–1401 [PubMed: 682044]

Staubli U, Schottler F, Nejat-Bina D (1987) Role of dorsomedial thalamic nucleus and piriform cortex in processing olfactory information. Behav Brain Res 25(2):117–129 [PubMed: 3675824]

Stockli J, Fazakerley DJ, James DE (2011) GLUT4 exocytosis. J Cell Sci 124(Pt 24):4147–4159. 10.1242/jcs.097063 [PubMed: 22247191]

Sundberg H, Doving K, Novikov S, Ursin H (1982) A method for studying responses and habituation to odors in rats. Behav Neural Biol 34(1):113–119 [PubMed: 7073634]

Suzuki N, Bekkers JM (2006) Neural coding by two classes of principal cells in the mouse piriform cortex. J Neurosci 26(46):11938–11947. 10.1523/JNEUROSCI.3473-06.2006 [PubMed: 17108168]

Suzuki N, Bekkers JM (2010) Inhibitory neurons in the anterior piriform cortex of the mouse: classification using molecular markers. J Comp Neurol 518(10):1670–1687. 10.1002/cne.22295 [PubMed: 20235162]

Thiebaud N, Johnson MC, Butler JL, Bell GA, Ferguson KL, Fadool AR, Fadool JC, Gale AM, Gale DS, Fadool DA (2014) Hyperlipidemic diet causes loss of olfactory sensory neurons, reduces olfactory discrimination, and disrupts odor-reversal learning. J Neurosci 34(20):6970–6984. 10.1523/JNEUROSCI.3366-13.2014 [PubMed: 24828650]

Tucker K, Cho S, Thiebaud N, Henderson MX, Fadool DA (2013) Glucose sensitivity of mouse olfactory bulb neurons is conveyed by a voltage-gated potassium channel. J Physiol 591(Pt 10):2541–2561. 10.1113/jphysiol.2013.254086 [PubMed: 23478133]

Uchida N, Mainen ZF (2003) Speed and accuracy of olfactory discrimination in the rat. Nat Neurosci 6(11):1224–1229. 10.1038/nn1142 [PubMed: 14566341]

Unger J, McNeill TH, Moxley RT, White M, Moss A, Livingston JN (1989) Distribution of insulin receptor-like immunoreactivity in the rat forebrain. Neuroscience 31(1):143–157 [PubMed: 2771055]

Venner A, Karnani MM, Gonzalez JA, Jensen LT, Fugger L, Burdakov D (2011) Orexin neurons as conditional glucosensors: paradoxical regulation of sugar sensing by intracellular fuels. J Physiol 589(Pt 23):5701–5708. 10.1113/jphysiol.2011.217000 [PubMed: 22005675]

Verhagen JV, Wesson DW, Netoff TI, White JA, Wachowiak M (2007) Sniffing controls an adaptive filter of sensory input to the olfactory bulb. Nat Neurosci 10(5):631–639. 10.1038/nn1892 [PubMed: 17450136]

Wachowiak M, Shipley MT (2006) Coding and synaptic processing of sensory information in the glomerular layer of the olfactory bulb. Semin Cell Dev Biol 17(4):411–423. 10.1016/j.semcdb.2006.04.007 [PubMed: 16765614]

Wada A, Yokoo H, Yanagita T, Kobayashi H (2005) New twist on neuronal insulin receptor signaling in health, disease, and therapeutics. J Pharmacol Sci 99(2):128–143 [PubMed: 16210778]

Welker WI (1964) Analysis of sniffing of the albino rat. Behaviour 22(3–4):223–244

Wesson DW, Keller M, Douhard Q, Baum MJ, Bakker J (2006) Enhanced urinary odor discrimination in female aromatase knockout (ArKO) mice. Horm Behav 49(5):580–586. 10.1016/j.yhbeh.2005.12.013 [PubMed: 16448653]

Wesson DW, Donahou TN, Johnson MO, Wachowiak M (2008) Sniffing behavior of mice during performance in odor-guided tasks. Chem Senses 33(7):581–596. 10.1093/chemse/bjn029 [PubMed: 18534995]

Wesson DW, Varga-Wesson AG, Borkowski AH, Wilson DA (2011) Respiratory and sniffing behaviors throughout adulthood and aging in mice. Behav Brain Res 223(1):99–106. 10.1016/j.bbr.2011.04.016 [PubMed: 21524667]

Wilson DA (2000) Odor specificity of habituation in the rat anterior piriform cortex. J Neurophysiol 83(1):139–145. 10.1152/jn.2000.83.1.139 [PubMed: 10634860]

Wilson DA (2003) Rapid, experience-induced enhancement in odorant discrimination by anterior piriform cortex neurons. J Neurophysiol 90(1):65–72. 10.1152/jn.00133.2003 [PubMed: 12660351]

Wilson DA (2009a) Olfaction as a model system for the neurobiology of mammalian short-term habituation. Neurobiol Learn Mem 92(2):199–205. 10.1016/j.nlm.2008.07.010 [PubMed: 18678264]

Wilson DA (2009b) Pattern separation and completion in olfaction. Ann N Y Acad Sci 1170:306–312. 10.1111/j.1749-6632.2009.04017.x [PubMed: 19686152]

Wilson DA, Stevenson RJ (2003) The fundamental role of memory in olfactory perception. Trends Neurosci 26(5):243–247. 10.1016/S0166-2236(03)00076-6 [PubMed: 12744840]

Wilson DA, Sullivan RM (2011) Cortical processing of odor objects. Neuron 72(4):506–519. 10.1016/j.neuron.2011.10.027 [PubMed: 22099455]

Xu J, Wang P, Li Y, Li G, Kaczmarek LK, Wu Y, Koni PA, Flavell RA, Desir GV (2004) The voltage-gated potassium channel Kv1.3 regulates peripheral insulin sensitivity. Proc Natl Acad Sci USA 101(9):3112–3117. 10.1073/pnas.0308450100 [PubMed: 14981264]

Youngentob SL (2005) A method for the rapid automated assessment of olfactory function. Chem Senses 30(3):219–229. 10.1093/chemse/bji017 [PubMed: 15741600]

Youngentob SL, Mozell MM, Sheehe PR, Hornung DE (1987) A quantitative analysis of sniffing strategies in rats performing odor detection tasks. Physiol Behav 41(1):59–69 [PubMed: 3685154]

Zhou Y, Wang X, Cao T, Xu J, Wang D, Restrepo D, Li A (2017) Insulin modulates neural activity of pyramidal neurons in the anterior piriform cortex. Front Cell Neurosci 11:378 10.3389/fncel.2017.00378 [PubMed: 29234275]

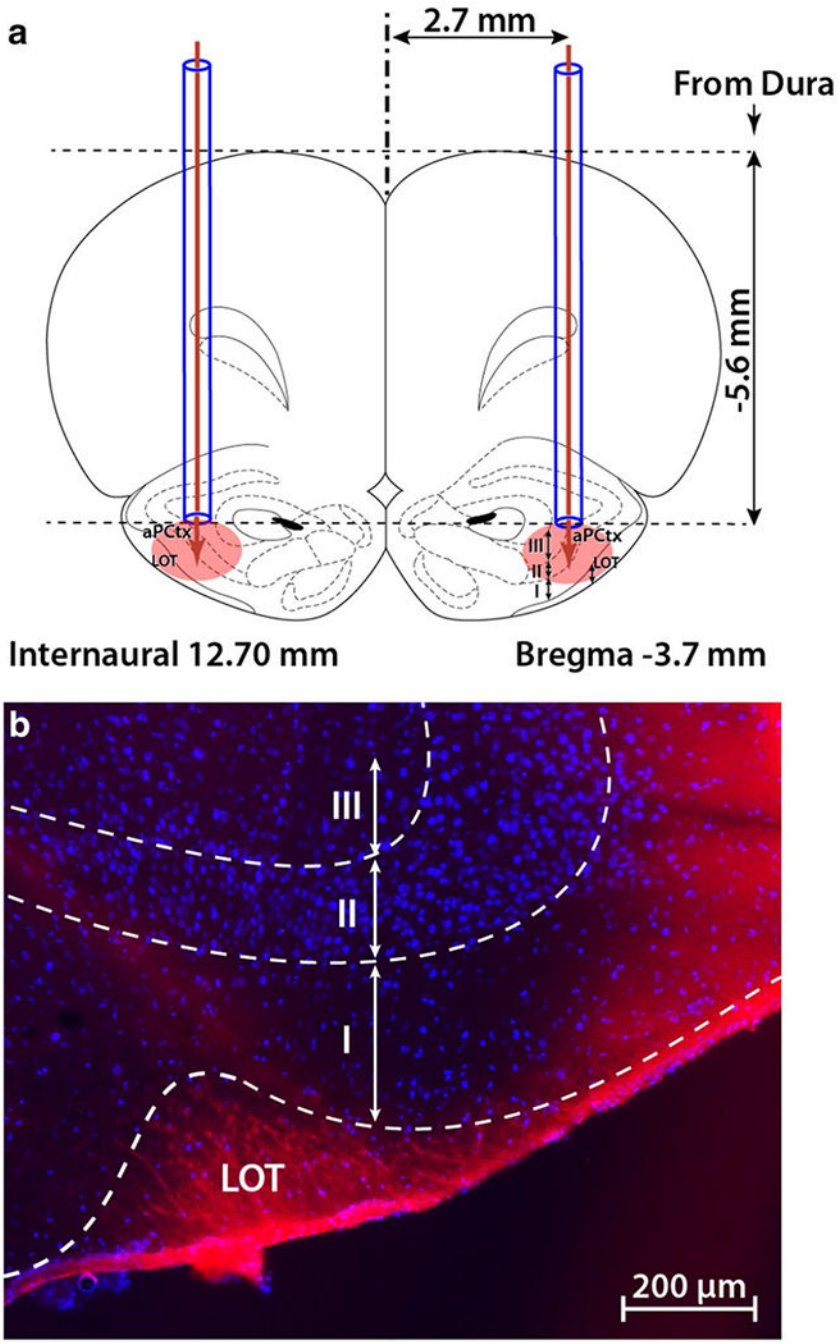


**Fig. 1.**

Site of intracranial injection in the anterior piriform cortex (aPCtx). **a** Two cannula guides were symmetrically implanted (coordinates: AP – 3.7 mm from Bregma, ML ± 2.7 mm and DV – 5.6 mm from dura), and 1 µl of drug or control vehicle (ACSF) was bilaterally injected (glucose, insulin, or MgTx). The coronal drawing was adapted from the Paxinos and Watson atlas (2007), plate 7. **b** A representative example of one brain section through the aPCtx, 30 min following the injection of 1 µl Evans blue. *LOT* lateral olfactory tract; *I, II, III* layers of the aPCtx; blue DAPI nuclear stain

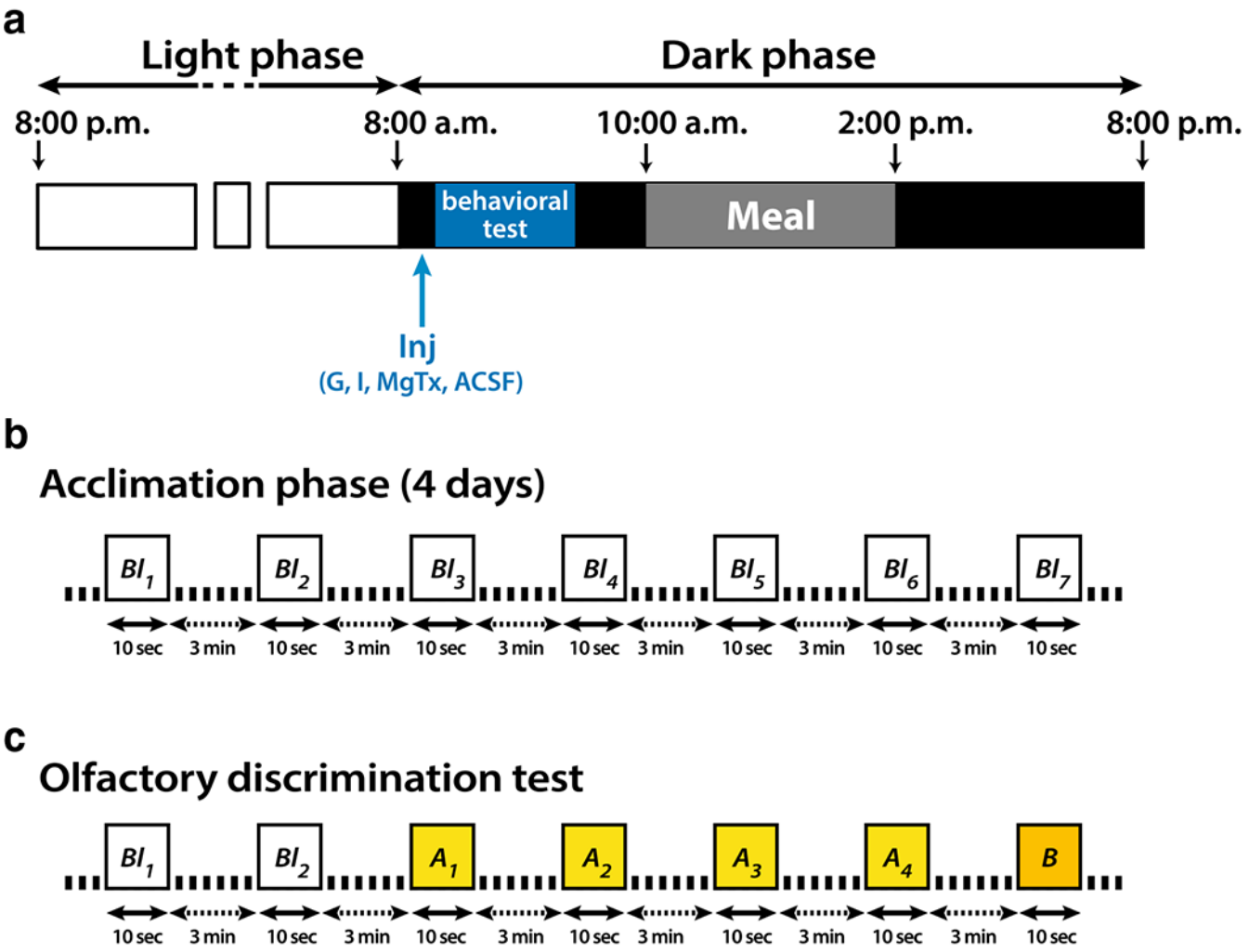


**Fig. 2.**

Non-invasive recording of sniff behavior. Schematic representation of the sound-attenuating dark chamber containing the whole-body plethysmograph (left) connected to a computer-operated olfactometer (right). The plethysmograph was composed of two independent airtight chambers: the reference chamber and the animal chamber. Air flux regularly crossed the animal chamber at a rate of 2 L/min and its composition was tightly controlled by the olfactometer. The pressure changes that resulted from animal respiration were measured by a differential pressure transducer (Model dpt, EMKA Technologies) with one sensor in the animal chamber and another in the reference chamber. The measured signal was amplified, digitally sampled at 1 kHz and acquired with a PC using an acquisition card (NI USB 6501, National Instrument, USA). In this experimental procedure, the olfactometer could deliver various stimuli: different percentages of 2 different odors (A and B: OdA, OdB) mixed with no odorized air, mixture of OdA and OdB at different ratios, and pure air (blank: Bl), using airflow regulators and solenoid valves. The animal behavior was monitored using two infrared cameras placed at two opposite corners of the sound-attenuating dark chamber

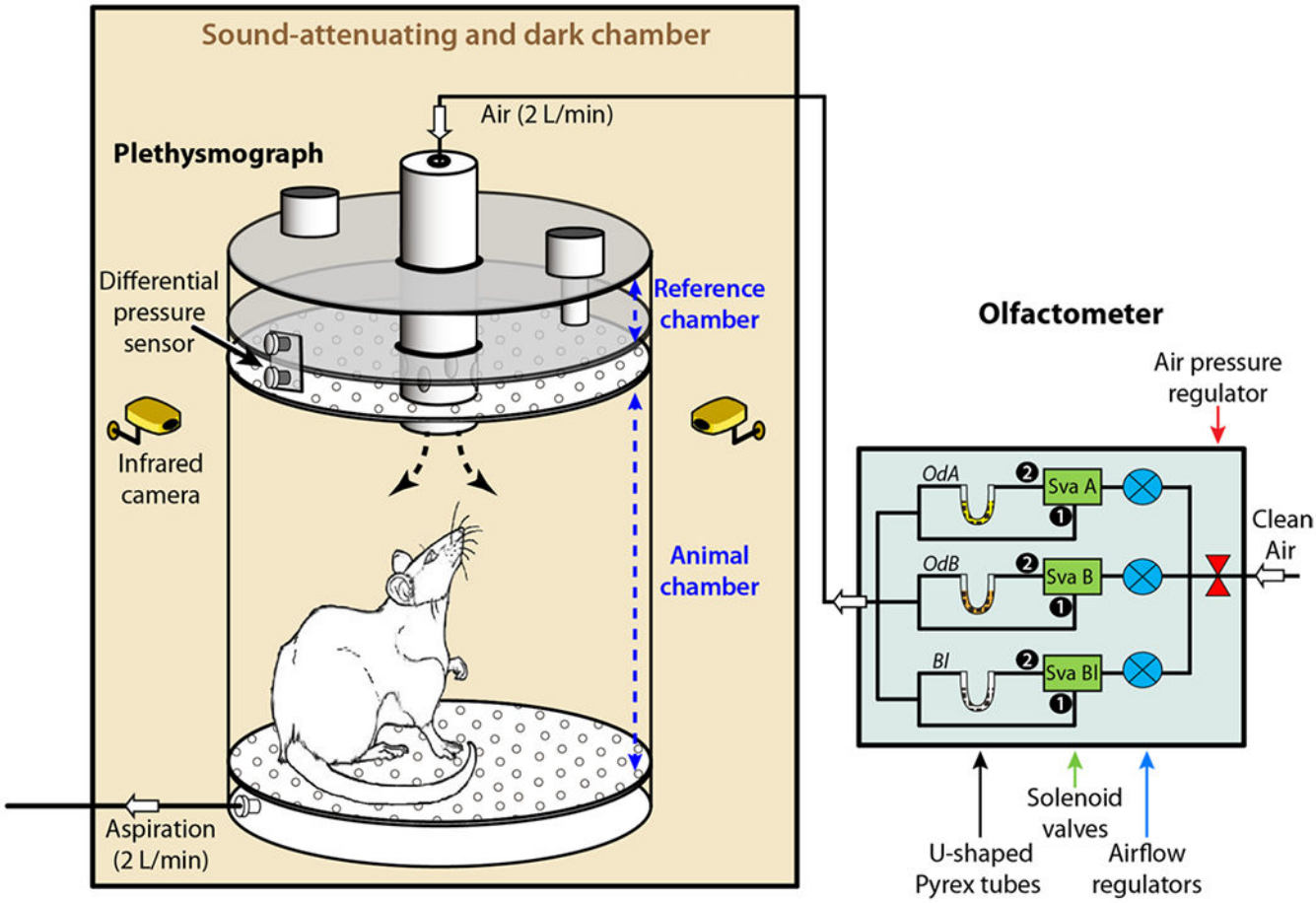


**Fig. 3.**

Schematic representation of the sniff behavior protocol (**a**), acclimation phase (**b**) and olfactory discrimination test (**c**). **a** Lights were turned off at 8:00 a.m. and rats had access to food from 11:00 a.m. to 3:00 p.m. Sniffing behavior was recorded continuously throughout the olfactory paradigm using a whole-body plethysmograph. **b** The rats were first allowed to habituate to the recording chamber for 4 days. Each day rodents received seven presentations of clean air (blank or Bl; Bl1 to Bl7). **c** Olfactory discrimination was measured using a cross-habituation task. The test began with two consecutive presentations of Bl then four consecutive presentations of an odorant (odor A, OdA1 to OdA4), followed by 1 presentation of a different odorant (odor B: OdB). Odor discrimination test was performed in the fasted state (before 10:00 a.m.) and just after injection (Inj) of 1 µl glucose (Gluc), insulin (Ins), margatoxin (MgTx) or artificial cerebral spinal fluid (ACSF) in the aPCtx. All odorants (Bl, OdA, OdB or mixture OdA/OdB) were presented for 10 s and were separated by 3 min

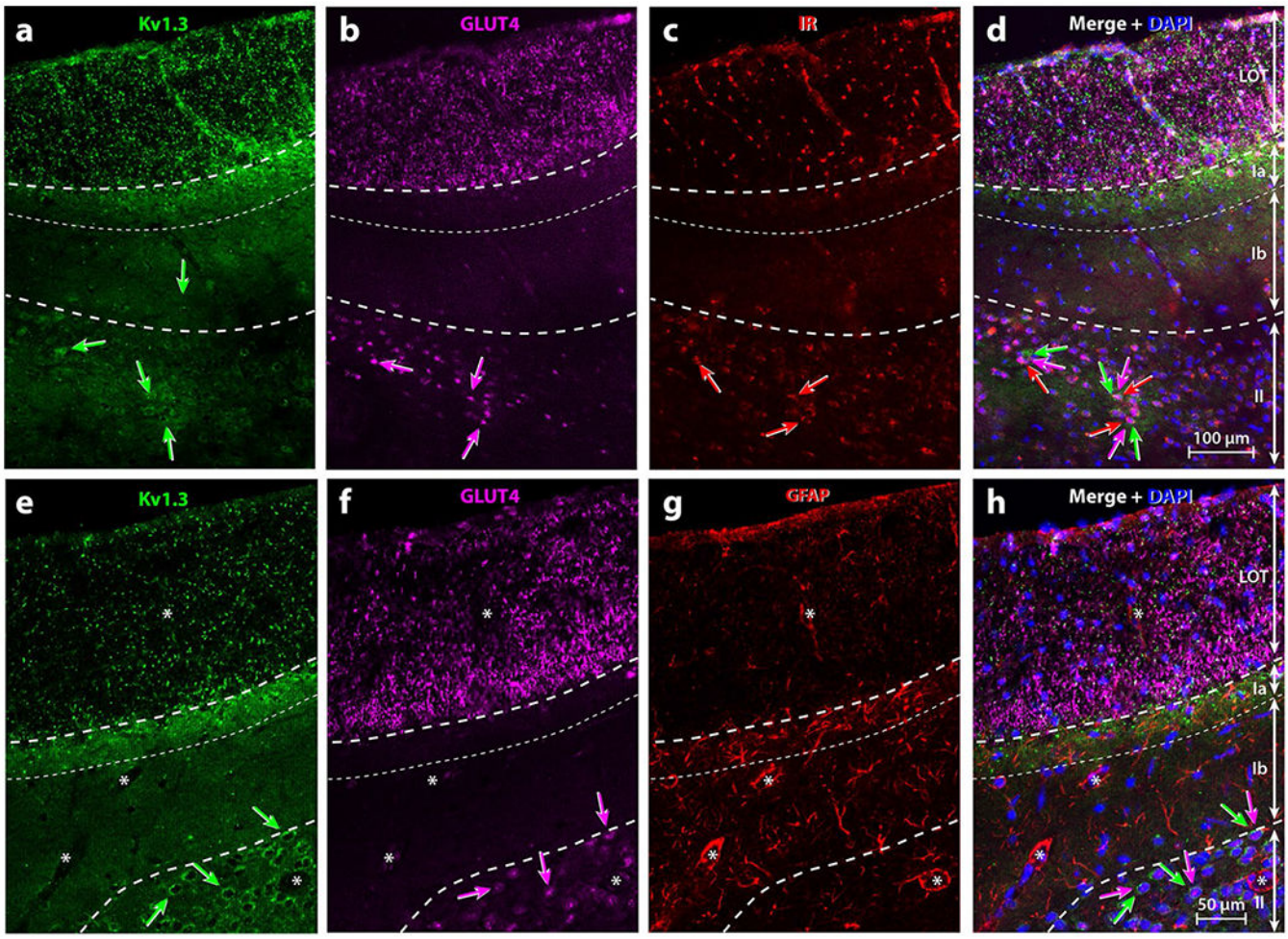


**Fig. 4.**

Representative triple-immunolabeling of metabolic signals within the rat anterior piriform cortex (aPCtx). Specific laminar location of (**a, e**) Kv1.3, (**b, f**) GLUT4, (**c**) IR, or (**g**) GFAP and their respective co-expression (Merge; **d, h**). Note: Kv1.3 and GLUT4 were abundant in the LOT while IR and GFAP labeling were less pronounced. Kv1.3 punctiform labeling was also present within Layer Ia where GFAP was more abundant. In Layer II, numerous neurons co-expressed Kv1.3, GLUT4 and IR (**a–f, h**; arrows with corresponding color) but not GFAP (**g**). Asterisks = blood vessels surrounded by GFAP-positive processes of astrocytes. *DAPI* blue nuclear stain; *LOT* lateral olfactory tract; *Ia, Ib, II* layers of the aPCtx delineated by dashed lines

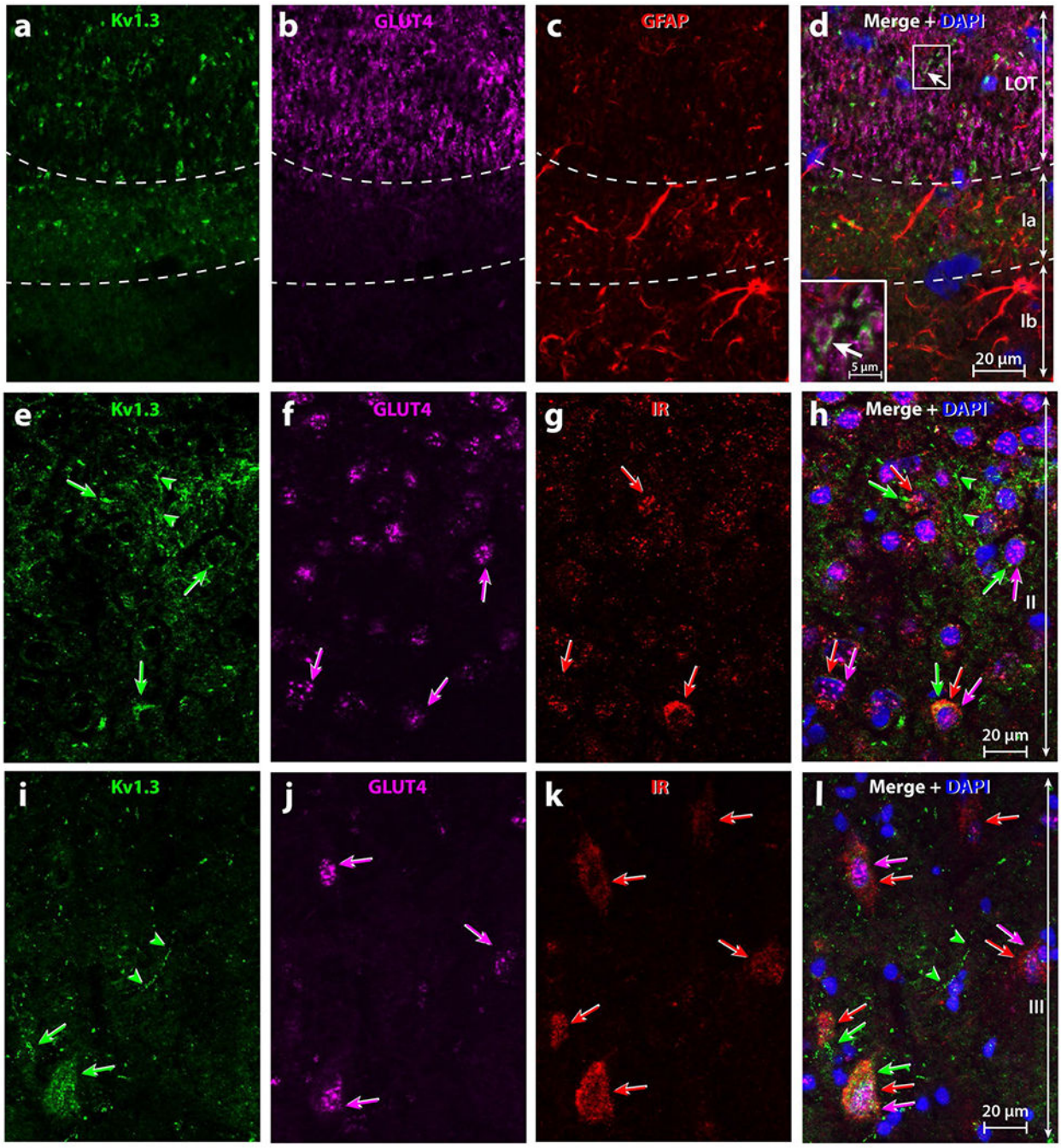


**Fig. 5.**

High magnification of triple-immunolabelling of metabolic signals within the rat anterior piriform cortex (aPCtx). Specific location of (**a, e, i**) Kv1.3, (**b, f, j**) GLUT4, (**c**) GFAP, and (**g, k**) IR and their respective co-expression (Merge, **d, h, l**). Images were acquired at high magnification in the LOT and Layer I (**a–d**), Layer II **e–h** and Layer III (**i–l**) of the aPCtx. In the LOT (**a–d**), Kv1.3 was located around the GLUT4 labeling (**d**, insert; arrow) and in Layer Ia inter-mingled with GFAP processes. In Layers II and III of the aPCtx (**e–l**), Kv1.3, IR, and GLUT4 were expressed within neuron cell bodies (arrows with corresponding

color). (**h, l**) Some neurons co-expressed two or three of these proteins, whereas others ones only one (1–3 arrows with corresponding color). Green arrow-heads processes expressing Kv1.3 only. *DAPI* blue nuclear stain; *LOT* lateral olfactory tract; *Ia, Ib, II* layers of the aPCtx delineated by dashed lines

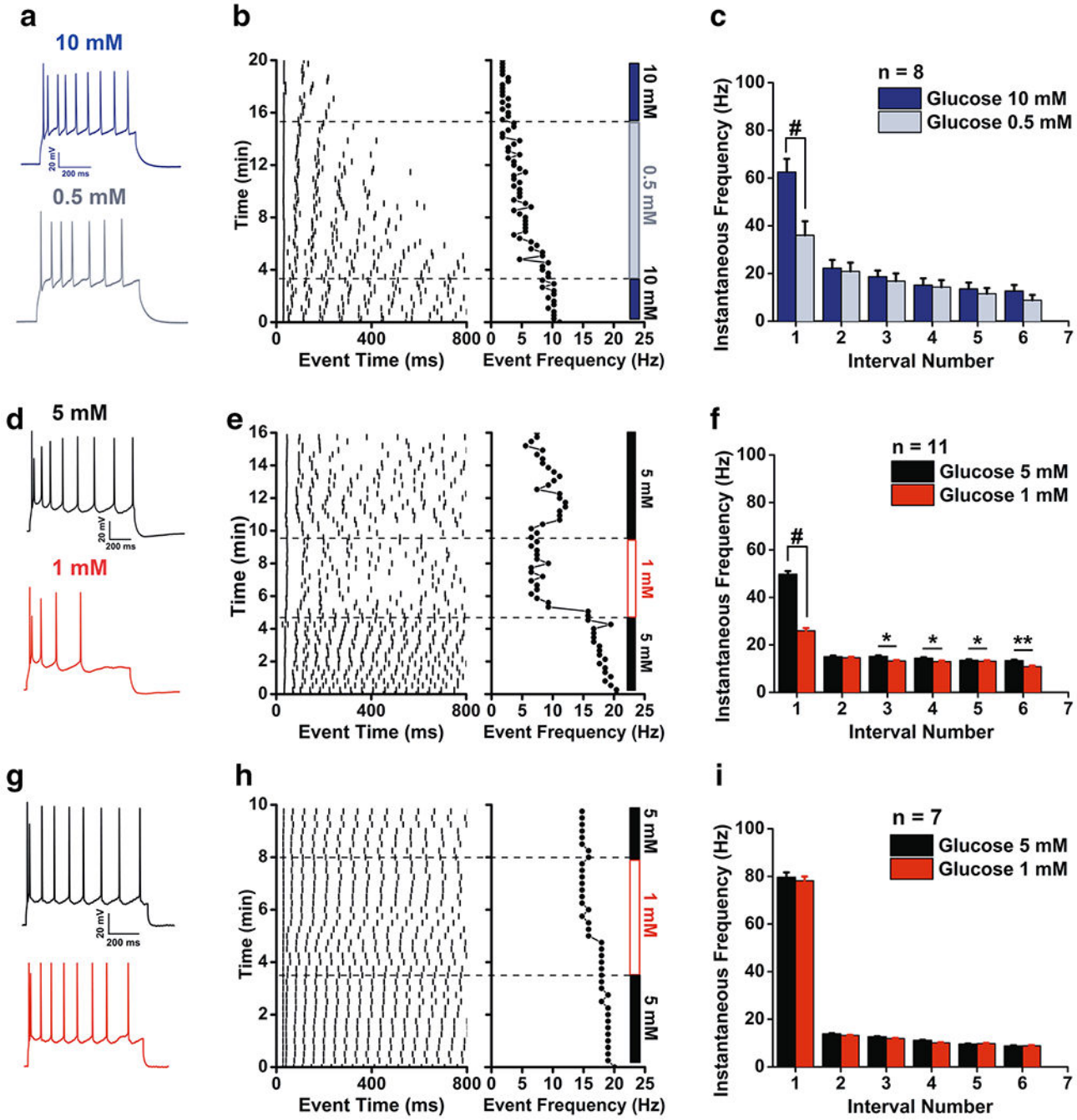


**Fig. 6.**

Glucose responsiveness of superficial pyramidal cells (SP) in the aPCtx. Representative whole-cell recordings acquired from SP cells at – 50 mV while evoking a train of 5 or more action potentials using a perithreshold current injection switched from (**a**) 10 mM vs. 0.5 mM glucose or (**d, g**) low, 5 mM vs. 1 mM glucose. Correlated raster plots for the representative recordings for (**b**) a glucose-excited cell in high glucose, (**e**) a glucose-excited and (**h**) a glucose-insensitive cell in low glucose. **c, f, i** Associated instantaneous frequency (IF) bar graphs for a population of SP cells recorded in (**c**) high or (**f, i**) low glucose, with

glucose excitation (**f**) and insensitivity subpopulations (**i**) respectively. Data represent mean ± standard error of the mean (SEM). Number of SP neurons recorded as noted. **c, f, i** 2-way RM ANOVA, with Bonferroni post-hoc test showing main effect for glucose concentration, $^{\#}p < 0.0001$, $^{*}p < 0.05$, $^{**}p < 0.01$

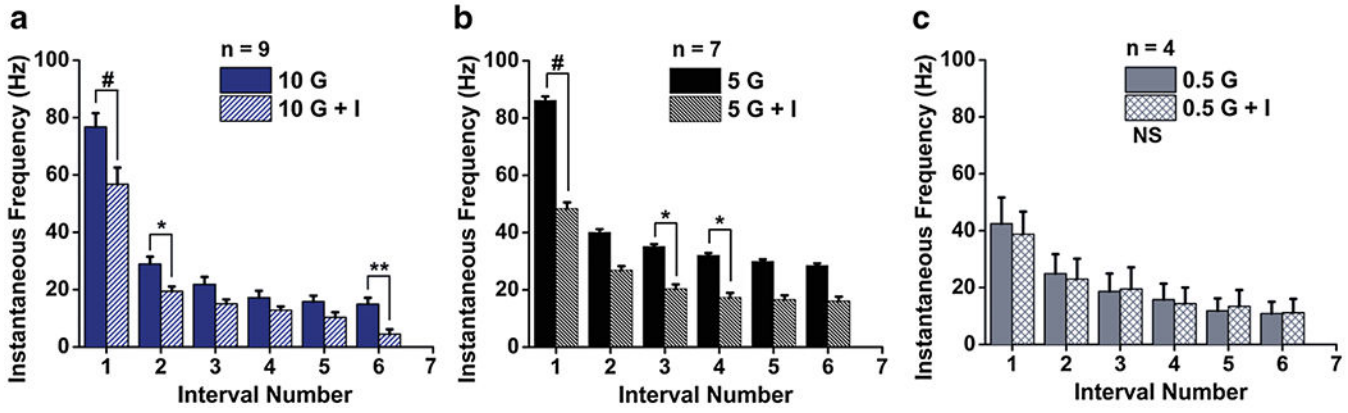


**Fig. 7.**

Insulin responsiveness of superficial pyramidal cells (SP) in the aPCtx. Summary of IF bar graphs generated as in Fig. 6 for a population of SP cells recorded at **a** high, 10 mM glucose (10 G) prior to the addition of insulin (10 G + I), **b** low, 5 mM glucose (5 G) prior to the addition *of* insulin (5 G + I), or trace, **c** 0.5 mM glucose (0.5 G) prior to the addition of insulin (0.5 G + I). two-way RM ANOVA, with Bonferroni post-hoc test showing main effect for treatment, $^{\#}p < 0.0001$, $^{*}p < 0.05$, $^{**}p < 0.01$, *NS* not significantly different

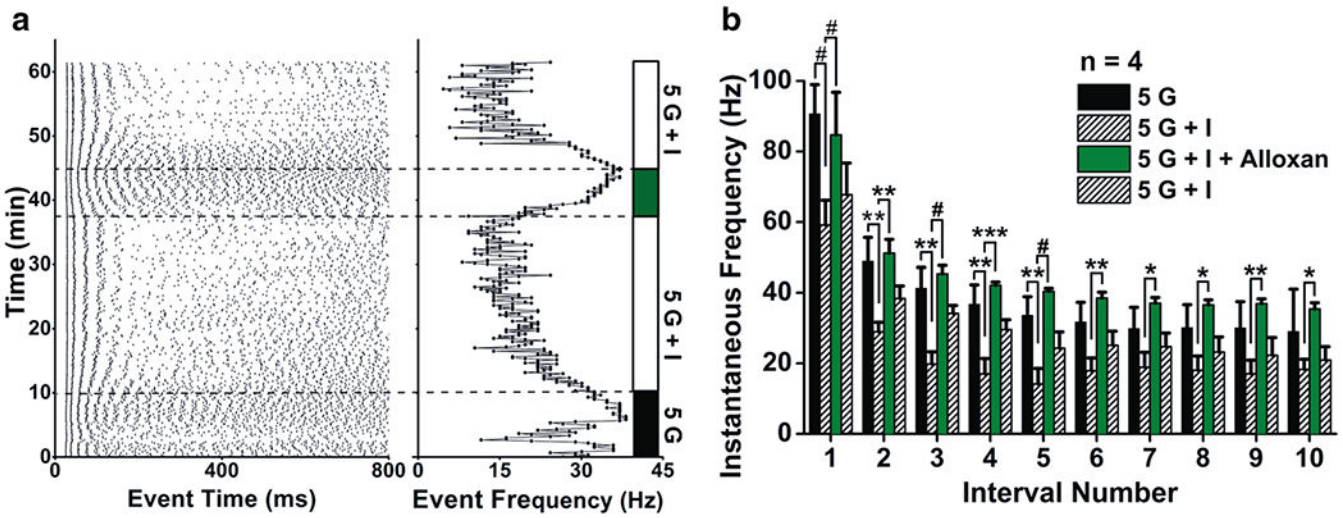


**Fig. 8.**

The selective glucokinase inhibitor, alloxan, blocks insulin-induced reduction of SP excitability and IF in SP cells. **a** Raster plot for a representative whole-cell recording as in Fig. 6b, e, h that was sequentially stimulated with bath application of 5 mM glucose (5 G; black bar), plus insulin (5 G + I; white bar), plus alloxan (5 G + I + A; grey bar), followed by washout (5 G + I; white bar). **b** Summary IF bar graph generated as in Fig. 6 for a population of SP cells that were sequentially stimulated with 5 mM glucose (5 G), plus insulin (5 G + I), plus alloxan (5 G + I + Alloxan), followed by washout (5 G + I). 2-way RM ANOVA, with Bonferroni post-hoc test showing main effect for treatment, $^{\#}p < 0.0001$, $^{*}p < 0.05$, $^{**}p < 0.01$, $^{***}p < 0.001$

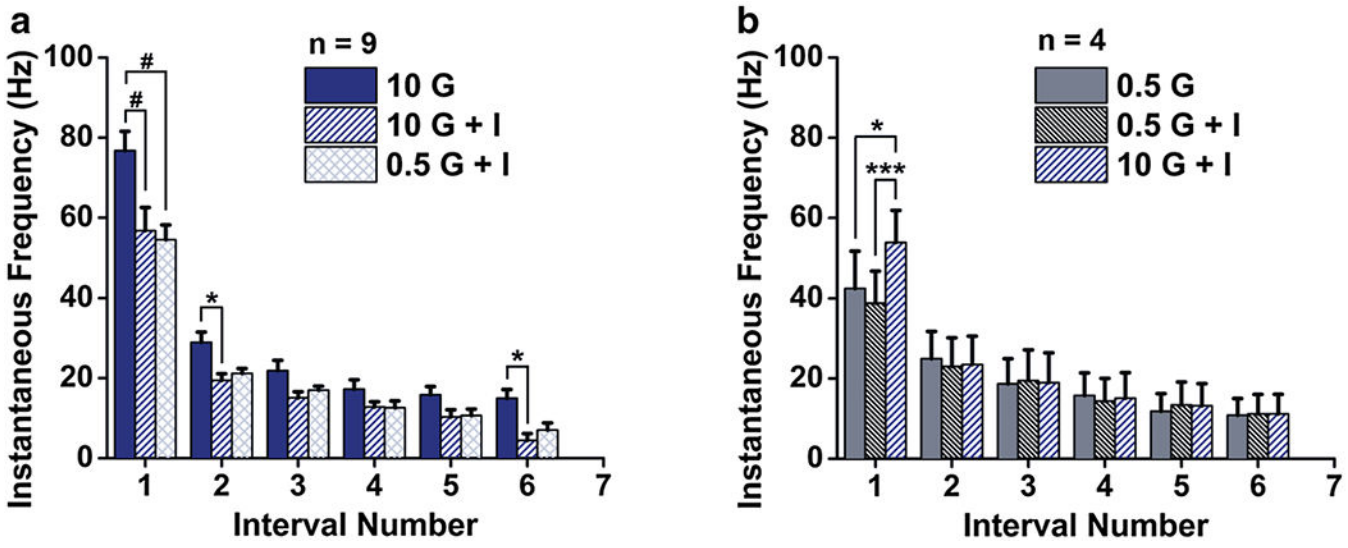


**Fig. 9.**

Insulin modulation of SP cells is glucose-concentration dependent. Summary IF bar graph generated as in Fig. 6 for a population of SP cells that were sequentially stimulated with glucose (G), plus insulin (G + I), followed by a change in glucose concentration. **a** Originating from high glucose (10 mM, 10 G) and changing to low glucose in the presence of insulin (5 mM, 0.5 G + I) and **b** originating from low glucose (0.5 G) and moving to high glucose in the presence of insulin (10 G + I). 2-way RM ANOVA, with Bonferroni post-hoc test showing main effect for treatment, $^{\#}p < 0.0001$, $^{*}p < 0.05$, $^{***}p < 0.001$

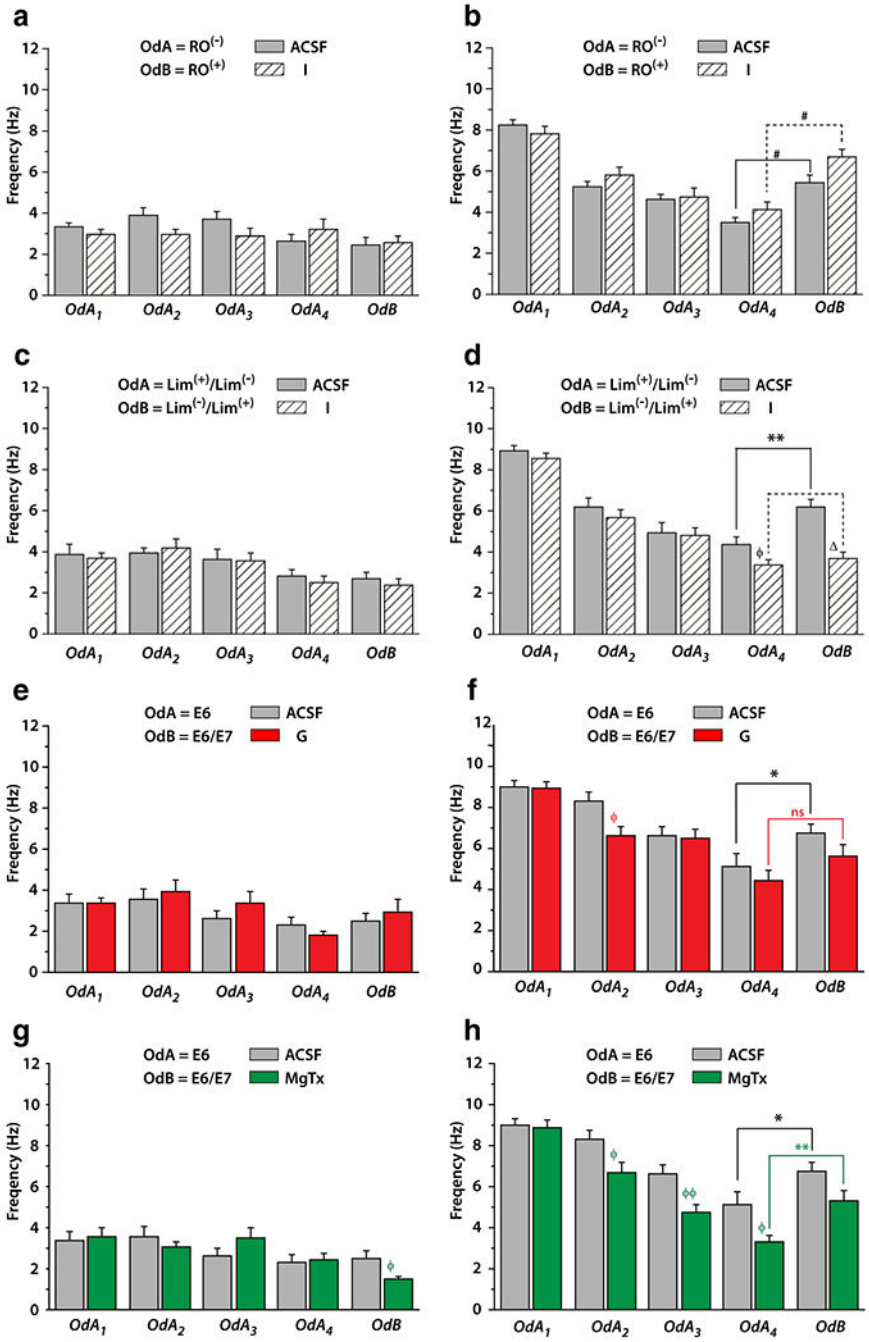


**Fig. 10.**

Effect of anterior piriform cortex (aPCtx) metabolic microinjections on sniffing frequency of rats during a cross-habituation paradigm. Bar graphs of the mean (± SEM) of rat respiratory frequency for each trial monitored (**a, c, e, g**) at steady state before each odor presentation and (**b, d, f, h**) during the five consecutive odor perceptions (four presentations of the same odor; OdA1 to OdA4 followed by a fifth and last odor presentation; OdB). Evolution of the sniffing frequency from OdA1 to OdA4 characterizes the habituation phase while data comparison between OdA4 and OdB allow the study the olfactory discrimination. Rats were

exposed (**a, b**) to RO/RO when micro-injected into the aPCtx with artificial cerebral spinal fluid (ACSF; gray bar, $n = 13$) or insulin (I; hatched bar, $n = 10$). (**c**, **d**) to 70% L/30% L and then 70% L/30% L when micro-injected into the aPCtx with ACSF, $n = 9$ or *I,* $n = 12$. **e**–**h** Same as **a, b** but rats were habituated with E6 and then to 70% E6/30% E7 after micro-injection into the aPCtx with (**e, f**) ACSF (gray bar, $n = 8$) or glucose (G; red bar, $n = 6$), or (**g, h**) with ACSF (gray bar, $n = 8$) or margatoxin (MgTx; green bar, $n = 8$). **a, c, e, g** For respiratory frequency steady state, a three-way RM ANOVA with injection, trail and bins as factors, shown no effect for micro-injection and any interaction between micro-injection and bins, micro-injection and trials or micro-injection, bins and trials. Comparison between MgTx and ACSF microinjection revealed a significant difference for the last trial (OdB) (**g**), Mann–Whitney test $\varphi\ p < 0.05$. For habituation phase, a three-way RM ANOVA completed by post hoc SNK, reveals for three type of OdA used (RO, **b**; L/L, **d**; E6, **f**–**h**) an effect for trial with for RO. An effect injection is demonstrated by SNK post hoc test or/and by Mann–Whitney U test for OdA4 (L/L; **d**) between I and ACSF microinjection, for OdA2 (E6; **f**) between G and ACSF and for OdA2 (E6; **h**) to OdA4 (E6) between MgTx and ACSF (Mann Whitney $U$ test, $^{\varphi}p < 0.05$, $^{\varphi\varphi}p < 0.01$). For discrimination comparison OdA4 vs. OdB a 3-way RM ANOVA shows, an effect for trial, for three type of used couple odorant, an effect micro-injection only for E6 vs. E6/E7 when MgTx injection is compared to ACSF and an interaction between trial, bins and injection for L/L vs. L/L. **b, g** Wilcoxon test shows significant increase in sniffing frequency between OdA4 vs. OdB for the two rats groups (**b**: injected ACSF and I and **g**: injected ACSF and MgTx). **d, f** Only ACSF injected rats increase sniffing frequency during OdB presentation